2015

# UNDERSTANDING BEHAVIOR OF PARTICLE STABILIZED EMULSIONS AND TRANFORMATIONS IN COLLOIDAL SYSTEMS

Amitesh Saha
*University of Rhode Island*, saha.tesh@gmail.com

# UNDERSTANDING BEHAVIOR OF PARTICLE STABILIZED EMULSIONS AND TRANFORMATIONS IN COLLOIDAL SYSTEMS

BY

AMITESH SAHA

A DISSERTATION SUBMITTED IN PARTIAL FULFILLMENT OF THE REQUIREMENTS FOR THE DEGREE OF

DOCTOR OF PHILOSOPHY

IN

CHEMICAL ENGINEERING

UNIVERSITY OF RHODE ISLAND

2015

DOCTOR OF PHILOSOPHY IN CHEMICAL ENGINEERING

OF

AMITESH SAHA

APPROVED:

Thesis Committee:

Major Professor Arijit Bose

Richard Brown

Mindy Levine

Anubhav Tripathi

Nasser H. Zawia
DEAN OF THE GRADUATE SCHOOL

UNIVERSITY OF RHODE ISLAND
2015

## ABSTRACT

Practically irreversible attachment of partially wettable particles to liquid-liquid interfaces presents an effective strategy for dispersing oil as stable drops in water column in the event of an oil spill. We investigate the potentials of using carboxyl-terminated carbon black particles for stabilizing oil-in-water emulsions motivated by the need for developing alternative dispersants. These particles on exposure to either acid or salt, become partially hydrophobic and stabilize emulsions which remain stable for months. Once at the interface, these particles can adsorb naphthalene, a potentially toxic polycyclic aromatic hydrocarbon and reduce its transport into the aqueous phase. Stable crude oil-in-sea water emulsions are formed using these CB particles (with no added acid or salt). These attributes make these particles a viable alternative or supplement to conventional dispersants for oil spill remediation.

While partially wettable particles are known to stabilize emulsions, we report a new strategy for stabilizing emulsions using very hydrophilic and hydrophobic particles which are otherwise incapable of forming emulsions alone. When such a hydrophilic and a hydrophobic particle suspension are mixed, attractive van der Waals interactions between the particles cause them to assemble at the oil-water interfaces into supraparticle aggregates that are partially wettable in both phases and stabilize emulsions. Van der Waals interaction energy between two particle types across an aqueous-organic interface provide a systematic guide to particle and liquid combinations that can be used for stabilizing emulsions using our strategy. A combination of optical microscopy, cryogenic electron microscopy and zeta potential measurements are used for these studies.

Time-resolved cryogenic transmission electron microscopy (TR-cryo-TEM) is used to investigate early stages of gypsum formation from a supersaturated solution of calcium sulfate hemihydrate. Our results indicate that a multi-step particle formation model, where an amorphous phase forms first, followed by transformation into a crystalline product, is applicable even at time scales of the order of tens of seconds for this system. Addition of a small amount of citric acid significantly delays reorganization to gypsum crystals due to complexation of available calcium ions with carboxylic groups. This induces disorder, and extends the time over which amorphous phase exists. Information about phase and morphology is obtained by energy dispersive X-ray spectroscopy (EDX) and selected area electron diffraction (SAED). Complementary X-ray diffraction experiments confirm our observations. Direct imaging of transient nanoscale samples by TR-cryo-TEM is a powerful technique for fundamental understanding of crystallization, and manyother evolving systems.

We have also used cryo-TEM to understand the impact of perfume raw materials (PRMs) on the evolution of microstructures in vesicular dispersions of commercial fabric softener Ultra Downy Free (UDF). While a ‘good’ perfume keeps the inherent micro structures intact, a ‘bad’ perfume triggers a series of changes which results in bilayer fragmentation and transition from multi lamellar vesicles to predominantly unilamellar structures. The behavior of bad perfume, eugenol is attributed to its interaction with the surfactant bilayer as confirmed by nuclear magnetic resonance experiments. This understanding can be exploited to screen PRMs which provide both pleasant odor over an extended period of time and also do not impact the stability of vesicular dispersions.

## ACKNOWLEDGMENTS

First and foremost I offer my sincerest gratitude to my major advisor Dr. Arijit Bose, for his valuable guidance and encouragement throughout my thesis. I am grateful to him not only for his support, but also his patience, wisdom whilst providing me the room to think and work independently. It was his constant motivation that made me push boundaries and explore the frontiers of colloids and material science.

I take this opportunity to thank my thesis committee members Dr. Anubhav Tripathi, Dr. Mindy Levine and Dr. Richard Brown for their valuable insights on my research projects. I would also like to thank my collaborators Dr. Vijay T. John at Tulane university and Dr. Marc Mamak at Procter & Gamble, Cincinnati, Ohio for their help and input. Jibao He at Tulane University trained me in using cryogenic scanning electron microscope and I am grateful to him for sharing his knowledge. I thank all my lab mates and fellow graduate students for their cooperation and valuable discussions on our research. I am grateful to National Science Foundation, Gulf of Mexico Research Initiative, Procter & Gamble and the University of Rhode Island Graduate Fellowship program for funding and supporting my doctoral work. The department of chemical engineering and its staffs Sheryl, Brenda and Rob have helped me enormously throughout my stay at URI. I thank them for their support and guidance at times when it is tough for a new student to adjust to a new country and culture.

Finally, I thank my parents for their unconditional love, support and faith in me which has made me what I am today.

## PREFACE

This thesis is written in manuscript format. The first chapter is a general introduction that covers some key topics extensively used throughout the thesis. The second chapter entitled "Oil Emulsification Using Surface-Tunable Carbon Black Particles" has been published on March 15, 2013 in ACS Applied Materials & Interfaces (*ACS Appl. Mater. Interfaces*, 2013, 5 (8), pp 3094–3100). Third chapter of this thesis entitled "In situ Assembly of Hydrophilic and Hydrophobic Nanoparticles at Oil-Water Interfaces as a Versatile Strategy to form Stable Emulsions" is currently under review at ACS Nano. The fourth chapter entitled "New Insights into the Transformation of Calcium Sulfate Hemihydrate to Gypsum Using Time-Resolved Cryogenic Transmission Electron Microscopy" has been published on July 2, 2012 in the journal Langmuir (*Langmuir*, 2012, 28 (30), pp 11182–11187). The fifth and final chapter of this thesis entitled "Understanding Impact of Perfume Raw Materials on the Evolution of Microstructures in Vesicular Dispersions relevant to Fabric Softeners" is in preparation for publishing in the journal Langmuir.

## TABLE OF CONTENTS

## LIST OF TABLES

## LIST OF FIGURES

*Chapter 3*

# CHAPTER 1

## 1.1 Introduction

### 1.1.1 Particle Stabilized Emulsions

Dispersing one liquid as tiny drops in another immiscible liquid generates emulsions. This is often achieved either by adding amphiphilic molecules like surfactants or partially wettable solid particles to the system. While surfactants lower interfacial surface tension and reduce the free energy for emulsification, particles driven by their preference to reside at the liquid-liquid interfaces result in emulsion stabilization.[1] Emulsions have wide range of applications in a variety of fields including drug delivery, novel material fabrication, oil recovery, cosmetics, food, paper, paint and personal products. [2-9] Their stability against coalescence over an extended duration if time is responsible for various interesting uses.

Emulsions stabilized solely by solid particles were first observed by Ramsden[10] and Pickering[11]. Better understanding of impact of particle shape, size, wettability and interfacial particle concentration on emulsion stability has helped in advancement of this field. Detachment energy, $\Delta E$, for a model spherical particle from a liquid-liquid interface into either bulk phase, is given by

$$\Delta E = \pi R^2 \gamma_{ow} (1 - |\text{Cos } \theta|)^2. \qquad (1)$$

Here R is the particle radius, $\gamma_{ow}$ is the oil-water interfacial tension and $\theta$ is the contact angle through either phase. For a typical oil-water interfacial tension of 35mN/m and R = 10nm, $\Delta E > 500$ kT for $55^\circ < \theta < 125^\circ$. This is illustrated in Fig. 1. Particles with these contact angles are partially wettable in both phases, and once at the interface, they would irreversibly attach to it and stabilize emulsion droplets.[12, 13] Once at the

oil-water interface, these particles can suppresses drop-drop coalescence and enhances emulsion stability. This is attributed to the fact that particles can be charged, providing repulsive barrier against coalescence between droplets, they can provide steric barriers,[8, 14] bridge across neighboring emulsion drops, and can retard the thinning of intervening liquid layer as drops approach each other[15, 16] because of enhanced interfacial viscosity.

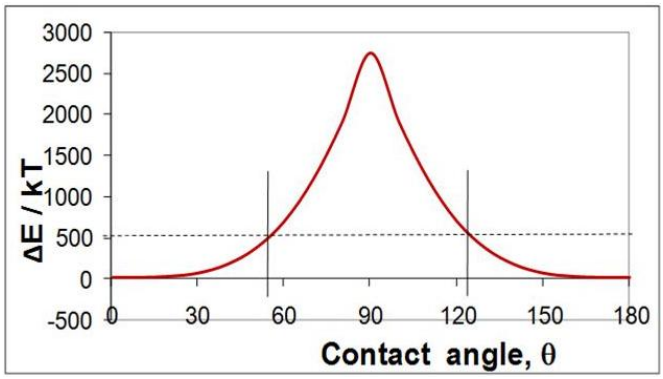


**Figure 1.** Detachment energy of a spherical particle from oil-water interface as a function of contact angle.

Intrinsic physical and chemical properties of particles can be exploited for creating emulsion drops with multifunctional properties – an attribute that separates it from surfactant stabilized emulsions. Another frontier that is exceedingly resorting to particle based emulsification technologies for better performance and environmental preservation is dispersant development for oil spill remediation. The Deepwater Horizon oil spill at the Gulf of Mexico in 2010 resulted in a release of about 5 million barrels[9] of crude oil and about 2 million gallons of surfactant based dispersants-Corexit 9500 A and Corexit 9527 were used to contain the spill. Dispersants break the spilled oil into tiny drops so that they can remain suspended in water column for extended periods of time to be degraded by bacteria. The use of surfactants as dispersants has been primarily driven by their effectiveness in emulsification and low

cost. However, inability of these surfactants in stabilizing oil indefinitely in large quantity of sea water coupled with their toxic impact[17] towards marine environment has prompted investigation of particles as dispersants.

Particle stabilized emulsions while effective, rely primarily on wettability of particles. Partially wettable particles are considered to be very good emulsifiers.[1, 18] However, a consequence of this partial wettability is that these particles will have a tendency to agglomerate or form a network in the phase they are suspended in, to minimize the overall free energy. Agglomeration often causes the particles to sediment, while network formation results in a large increase of zero shear viscosity.[1, 19] Generally, for creating a homogeneous dispersion of individual partially wettable particles for emulsification requires sustained input of energy up to the time a second immiscible liquid is introduced to the system. Some of these features have resulted in less usage of particles as emulsion stabilizers despite of their enormous potentials[9] for different applications which usually require less energy intensive processes. This has prompted a search for novel strategies to stabilize emulsions using particles[14] to exploit their unique properties.

A focus of this thesis is to study behavior of particles at liquid-liquid (oil-water) interfaces with the goal of developing particle based, alternative dispersants for emulsification of oil subsequent to a surface or sub-sea level oil spill. As a supplement to this, possibility of developing a new energy efficient strategy for forming particle stabilized emulsions that can be used to combine particles of different functionalities at emulsion droplet surfaces or generating novel materials is also explored.

### 1.1.2 Early Stages of Crystallization

Crystallization from supersaturated solution has been studied extensively. However, very little is known about the early stages of particle formation. Understanding these early stages is very crucial as it dictates the existence of subsequent phases and morphologies. This becomes more important when additives are to be rationally designed to modulate the crystallization process, as interaction of additive molecules with precursors are known to happen at very early stages. Classical nucleation theory predicts that the earliest particles that form have the crystal structure of the end product. On the other hand, models systems[20-23] have described formation of disordered clusters that result in reorganization to ordered crystalline domains. Crystallization of inorganic salts[24-26] have shown that transitions in precursor phases occur at very early time points. Hence, it is important to understand the pathway through which crystallization proceeds. Fig. 2 illustrates some interesting questions.

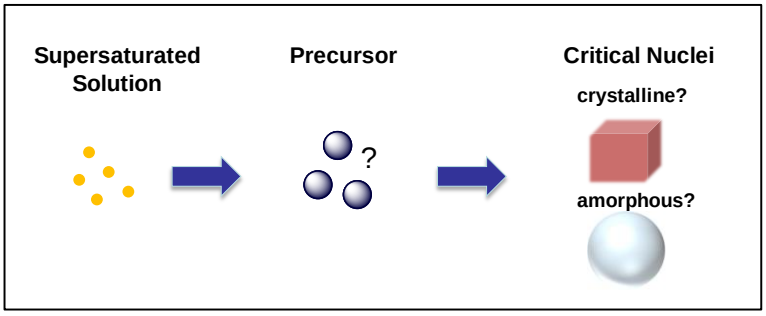


**Figure 2.** Schematic showing possible pathways for the onset of crystallization.

Techniques like Light microscopy, scanning electron microscopy, differential scanning calorimetry and atomic force microscopy have traditionally been deployed to understand crystallization. However, their inability to probe transitions at very early time points have left many questions unanswered. Time resolved cryogenic transmission electron microscopy (TR cryo TEM) is a technique that provides the

ability to quench samples in their native environment – hence preserving phase and morphology information. It provides direct real time imaging capability for transitioning systems and can be used to probe short time scales and very small length scales.

Early stages of gypsum crystallization from a supersaturated solution is investigated using TR cryo TEM. For this we carefully investigate the crystallization process to capture transitions that happen over short period of time. Impact of additives on the crystallization process is also explored. This understanding is crucial not only for unraveling the steps involved in crystallization process, but also to implement these in processes which need well control of crystal or particle properties for specific uses such as in plaster and building industries,[27] scaling control in pipes, heat exchangers, desalination plants [28,29, 30] and pharmaceutical industry.

### 1.1.3 Vesicles

Vesicles are formed when bilayers close back on themselves, because an open sheet-like configuration would involve a large energy along the hydrophobic edges in contact with the aqueous environment.[31] This results in encapsulation of aqueous environment. These vesicles can be uni- or multilamellar. Fig.3 shows a schematic of a multilamellar vesicle. Vesicle dispersions find use in drug delivery, cosmetics, fabric softeners etc. Double tailed cationic surfactants are the chief ingredients of fabric softeners which result in vesicles. These surfactants at the last rinsing step of wash cycle are adsorbed on negatively charged textiles and results in lubricating action relevant to fabric softening.[32]

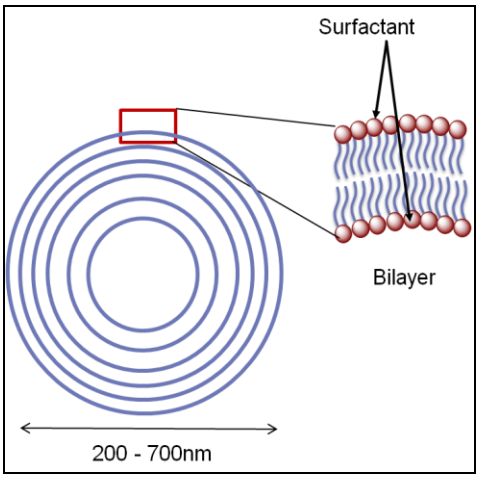


**Figure 3.** Schematic representation of a multilamellar vesicle showing a typical arrangement of surfactants in the bilayer.

Fragrance is an integral part of these consumer good products and extended duration of smell is an important product requirement as it determines acceptability by consumers. For this purpose, perfume is added to vesicular dispersions - a key constituent of many consumer products. However addition of a foreign molecule to a stable dispersion of vesicles can result in structural and morphological changes which can either destabilize a formulation by changes in rheology or decrease efficacy of product due to changes in microstructures. [33, 34] Hence, understanding changes induced by different perfume raw materials(PRMs) is a key to screening 'good' and ' bad' fragrance. Efforts to understand impact of PRMs on vesicular dispersions using techniques like selected ion flow tube mass spectrometry (SIFT-MS)[35] have not yielded in complete unraveling of the dynamics involved in these processes. Insight into this process also has implication for understanding transitions induced by hydrophobic additives in self assembled surfactant based colloidal systems.

Vesicular dispersion of commercial fabric softener Ultra Downy Free (UDF) is exposed to different PRMs and a combination of time resolved cryogenic transmission

electron microscopy, nuclear magnetic resonance is used to explore microstructural changes and specific interactions with surfactant bilayer. Real time information about structures quenched in sample coupled with insights into molecular interactions at the bilayer, shed light into the mechanism by which PRMs influence over all properties of vesicular dispersions.

**References**


1. Binks, B. P., Horozov, T. S., *Colloidal Particles at Liquid Interfaces*. Cambridge University Press: 2008.

2. Frelichowska, J.; Bolzinger, M.-A.; Pelletier, J.; Valour, J.-P.; Chevalier, Y., Topical delivery of lipophilic drugs from o/w Pickering emulsions. *International Journal of Pharmaceutics* **2009,** 371, (1-2), 56-63.

3. Velev, O. D.; Furusawa, K.; Nagayama, K., Assembly of Latex Particles by using Emulsion Droplets as Templates. 1. Microstructured Hollow Spheres. *Langmuir* **1996,** 12, (10), 2374-84.

4. Hong, L.; Jiang, S.; Granick, S., Simple Method to Produce Janus Colloidal Particles in Large Quantity. *Langmuir* **2006,** 22, (23), 9495-9499.

5. Sullivan, A. P.; Kilpatrick, P. K., The Effects of Inorganic Solid Particles on Water and Crude Oil Emulsion Stability. *Industrial & Engineering Chemistry Research* **2002,** 41, (14), 3389-3404.

6. Lee, M. N.; Chan, H. K.; Mohraz, A., Characteristics of Pickering Emulsion Gels Formed by Droplet Bridging. *Langmuir* 28, (6), 3085-3091.

7. Rousseau, D., Fat crystals and emulsion stability - a review. *Food Research International* **2000,** 33, (1), 3-14.

8. Tambe, D. E.; Sharma, M. M., The effect of colloidal particles on fluid-fluid interfacial properties and emulsion stability. *Advances in Colloid and Interface Science* **1994,** 52, 1-65.

9. Saha, A.; Nikova, A.; Venkataraman, P.; John, V. T.; Bose, A., Oil Emulsification Using Surface-Tunable Carbon Black Particles. *ACS Applied Materials & Interfaces* **2013,** 5, (8), 3094-3100.

10. Ramsden, W., The separation of solid materials on the surface of solutions and suspensions. Observations concerning surface diaphragms, foam blisters, emulsions and mechanical coagulation. [machine translation]. *Proceedings of the Royal Society of London* **1903,** 72, 156-64.

11. Pickering, S. U., Emulsions. *Journal of the Chemical Society, Transactions* **1907,** 91, 2001-21.

12. Finkle, P.; Draper, H. D.; Hildebrand, J. H., The theory of emulsification. *Journal of the American Chemical Society* **1923,** 45, 2780-8.

13. Schulman, J. H.; Leja, J., Control of contact angles at the oil-water-solid interfaces. Emulsions stabilized by solid particles (barium sulfate). *Transactions of the Faraday Society* **1954,** 50, 598-605.

14. Binks, B. P., Particles as surfactants - similarities and differences. *Current Opinion in Colloid & Interface Science* **2002,** 7, (1,2), 21-41.

15. Nushtayeva, A. V.; Kruglyakov, P. M., Capillary pressure in a thinning emulsion film stabilised by spherical solid particles. *Mendeleev Communications* **2001**, (6), 235-237.

16. Kruglyakov, P. M.; Nushtayeva, A. V.; Vilkova, N. G., Experimental investigation of capillary pressure influence on breaking of emulsions stabilized by solid particles. *Journal of Colloid and Interface Science* **2004,** 276, (2), 465-474.

17. Rico-Martinez, R.; Snell Terry, W.; Shearer Tonya, L., Synergistic toxicity of Macondo crude oil dispersant Corexit 9500A(Â®) to the Brachionus plicatilis species complex (Rotifera). *Environmental pollution (Barking, Essex : 1987)* 173C, 5-10.

18. Binks, B. P.; Whitby, C. P., Silica Particle-Stabilized Emulsions of Silicone Oil and Water: Aspects of Emulsification. *Langmuir* **2004,** 20, (4), 1130-1137.

19. McGorty, R.; Fung, J.; Kaz, D.; Manoharan, V. N., Colloidal self-assembly at an interface. *Materials Today (Oxford, United Kingdom)* **2010,** 13, (6), 34-42.

20. Zhang, T. H.; Liu, X. Y., Nucleation: what happens at the initial stage? *Angewandte Chemie, International Edition* **2009,** 48, (7), 1308-1312.

21. Zhang, T. H.; Liu, X. Y., How Does a Transient Amorphous Precursor Template Crystallization. *Journal of the American Chemical Society* **2007,** 129, (44), 13520-13526.

22. Zhang, T. H.; Liu, X. Y., Multistep Nucleation: Kinetic Study Based on Colloidal Crystallization. *Journal of Physical Chemistry B* **2007,** 111, (50), 14001-14005.

23. Erdemir, D.; Lee, A. Y.; Myerson, A. S., Nucleation of Crystals from Solution: Classical and Two-Step Models. *Accounts of Chemical Research* **2009,** 42, (5), 621-629.

24. Rieger, J.; Frechen, T.; Cox, G.; Heckmann, W.; Schmidt, C.; Thieme, J., Precursor structures in the crystallization/precipitation processes of CaCO3 and

control of particle formation by polyelectrolytes. *Faraday Discussions* **2007,** 136, 265-277.

25. Pouget, E. M.; Bomans, P. H. H.; Goos, J. A. C. M.; Frederik, P. M.; de With, G.; Sommerdijk, N. A. J. M., The Initial Stages of Template-Controlled CaCO3 Formation Revealed by Cryo-TEM. *Science (Washington, DC, United States)* **2009,** 323, (5920), 1455-1458.

26. Pichon, B. P.; Bomans, P. H. H.; Frederik, P. M.; Sommerdijk, N. A. J. M., A Quasi-Time-Resolved CryoTEM Study of the Nucleation of CaCO3 under Langmuir Monolayers. *Journal of the American Chemical Society* **2008,** 130, (12), 4034-4040.

27. Middendorf, B.; Vellmer, C.; Schmidt, M., Take a closer look: Calcium sulphate based building materials in interaction with chemical additives. *Special Publication - Royal Society of Chemistry* **2004,** 292, (Nanotechnology in Construction), 263-272.

28. Weijnen, M. P. C.; Van Rosmalen, G. M., Adsorption of phosphonates on gypsum crystals. *Journal of Crystal Growth* **1986,** 79, (1-3, [Pt. 1]), 157-68.

29. Van Rosmalen, G. M.; Daudey, P. J.; Marchee, W. G. J., An analysis of growth experiments of gypsum crystals in suspension. *Journal of Crystal Growth* **1981,** 52, (2), 801-11.

30. Akyol, E.; Oner, M.; Barouda, E.; Demadis, K. D., Systematic Structural Determinants of the Effects of Tetraphosphonates on Gypsum Crystallization. *Crystal Growth & Design* **2009,** 9, (12), 5145-5154.

31. Israelachivili, J. N., *Intermolecular and surface forces*. Second ed.; Academic Press: 2005.

32. Obendorf, S. K.; Dixit, V.; Woo, D. J., Microscopy Study of Distribution of Laundry Fabric Softener on Cotton Fabric. *Journal of Surfactants and Detergents* **2009,** 12, (3), 225-230.

33. Seth, M.; Ramachandran, A.; Murch, B. P.; Leal, L. G., Origins of Microstructural Transformations in Charged Vesicle Suspensions: The Crowding Hypothesis. *Langmuir* **2014,** 30, (34), 10176-10187.

34. Branson, D. H.; Rajadhyaksha, S., Distribution of malathion on Gore-Tex fabric before and after sunlight exposure and laundering as determined by electron microscopy. *ASTM Special Technical Publication* **1988,** 989, (Perform. Prot. Clothing), 651-9.

35. Heynderickx, P. M.; De Clercq, S.; Saveyn, P.; Dewulf, J.; Van Langenhove, H., Determination of the sorption and desorption kinetics of perfume raw materials in the liquid phase with vesicular dispersion: Application of SIFT-MS. *Chemical Engineering Journal (Amsterdam, Netherlands)* **2013,** 217, 281-288.

# CHAPTER 2

## Oil Emulsification Using Surface-Tunable Carbon Black Particles

(published in ACS Applied Materials & Interfaces, 2013, 5 (8), pp 3094–3100)

*Amitesh Saha,[†] Ani Nikova,[ǂ] Pradeep Venkataraman,[§] Vijay T. John,[§] Arijit Bose[†*]*

† Department of Chemical Engineering, University of Rhode Island, Kingston, RI 02881, USA

ǂ Cabot Corporation, 157 Concord Road, Billerica, MA 01821, USA

§ Department of Chemical and Biomolecular Engineering, Tulane University, New Orleans, LA 70118, USA

*Corresponding author: Arijit Bose; tel: 401-874-2804, email: bosea@egr.uri.edu

## 2.1 Abstract

Emulsification of oil from a subsurface spill and keeping it stable in the water is an important component of the natural remediation process. Motivated by the need to find alternate dispersants for emulsifying oil following a spill, we examine particle-stabilized oil-in-water emulsions. Emulsions that remain stable for months are prepared either by adding acid or salt to carboxyl-terminated carbon black (CB) suspension in water to make the particles partially hydrophobic, adding the oil to this suspension and mixing. When naphthalene, a model potentially toxic polycyclic aromatic hydrocarbon, is added to octane and an emulsion formed, it gets adsorbed significantly by the CB particles, and its transport into the continuous water is markedly reduced. In contrast to an undesirable sea water-in-crude oil emulsion produced using a commercially used dispersant, Corexit 9500A, we demonstrate the formation of a stable crude oil-in-sea water emulsion using the CB particles (with no added acid or salt), important for natural degradation. The large specific surface area of these surface functionalized CB particles, their adsorption capability and their ability to form stable emulsions are an important combination of attributes that potentially make these particles a viable alternative or supplement to conventional dispersants for emulsifying crude oil following a spill.

## 2.2 Introduction

Surfactants are commonly used to stabilize emulsions. Their ubiquity for this application rests on their effectiveness and their low cost. A practical example is the ~1.8 million gallons of surfactant (Corexit 9500A and Corexit 9527) used for the

Deepwater Horizon oil spill in the Gulf of Mexico in 2010. For the subsurface application, the crude oil-in-sea water emulsion drops should be around 100 μm in diameter, and needed to stay stable in the water column for a few months for optimum consumption by bacteria. While effective, the exposure of the surfactant to the large quantity of sea water promoted its dissolution into the aqueous phase resulting in emulsion destabilization, rendering the oil less effective for natural remediation. This issue as well as the potentially negative consequences of the surfactant on the ecological chain[1] have prompted a search for alternate dispersants. Particles represent a different class of emulsion stabilizers, and they offer intriguing possibilities for this purpose. This is mainly driven by the fact that particles can adsorb almost irreversibly to liquid-liquid interfaces, allowing such emulsions to be stable even at extremely low concentrations of the dispersed phase. In addition, intrinsic surface, thermal, optical, electrical and magnetic properties of particles can be exploited to produce emulsions that have greater functionalities than surfactant stabilized ones. We exploit some of these features of particles in the work reported here.

Emulsions stabilized solely by solid particles were first observed by Ramsden[2] and Pickering.[3] Subsequent work investigated the relationship between the three phase contact angle and emulsion stability, [4, 5] and the effect of particle flocculation on emulsification.[6] Commercial uses of Pickering emulsions are not common, but potential application areas that take advantage of the properties of the particles are emerging, including drug delivery,[7] novel material fabrication,[8, 9] oil recovery,[10] cosmetics, food, paper, paint and personal products.[11-13] A range of particles including silica, polystyrene, iron oxide, bentonite clay and graphene oxide[14-22] have

been employed for emulsion formation. In each of these cases, the particle properties also play useful roles in determining the final characteristics of the emulsion.

Spontaneous entry of particles into liquid-fluid (termed oil-water for the remainder for this paper) interfaces is slow,[23] and mixing is used to accelerate this process. The energy $\Delta E$ required to detach a particle (we assume spherical particles for this illustration) from an oil-water interface into either bulk phase is given by

$$\Delta E = \pi R^2 \gamma_{ow} (1 - |\text{Cos } \theta|)^2, \quad (1)$$

where R is the particle radius, $\gamma_{ow}$ is the oil-water interfacial tension and $\theta$ is the contact angle through either phase. For $R$ = 50nm, $\gamma_{ow}$ = 30mN/m, and $\theta = 90°$, Eq.(1) gives $\Delta E \sim 5.7 \times 10^4 kT$. Therefore, once a particle is in the interface it will not detach spontaneously. The presence of particles at the oil-water interfaces suppresses drop-drop coalescence and enhances emulsion stability. This is because the particles can be charged, providing repulsive interactions between droplets,[24] they can bridge across neighboring emulsion drops, [25-27] [28] they can provide steric barriers[13, 29] and they can impart enhanced interfacial viscosity that retards the thinning of an intervening liquid layer as the droplets approach each other.[30, 31] Stable emulsions can be formed even if there is incomplete coverage of droplet surfaces.[20] [25] The interaction of particle charge with the charge on the oil-water interfaces affects the assembly of particles at these interfaces.[32-35] Interfacial particle concentrations,[13, 36] their size,[13, 37] shape[38] [39] and interparticle interactions[40, 41] impact the stability of these emulsions.[24]

Driven by their easy availability, range of surface chemistry, biocompatibility, high specific surface area, their ability to adsorb organics, their classification as GRAS (generally regarded as safe) materials and their fractal nature, we have used a

commercially available grade of surface modified carbon black (CB) particles suspended in water, to create, and examine in detail, particle-stabilized octane-in-water emulsions. The presence of the emulsifier particles in the aqueous phase is expected to promote the formation of oil-in-water emulsions. The CB particles are aggregates of 8-10 'primary' particles, each of diameter ~20nm, fused together in a flame process. The resulting fractal particle is about 100nm-200nm in nominal size and has a specific surface area of approximately $200m^2/g$. CB particles are used as reinforcement in rubber tires, as pigments in inks and in thermoplastics for enhanced electrical conductivity, Young's modulus and UV stability.[42, 43] Carbon blacks have been used previously as an emulsifier, but their inherent hydrophobicity causes them to form water-in-oil emulsions. In this work, we take advantage of covalently linked surface groups that can be used to tune the CB hydrophilicity, to consistently form oil-in-water emulsions. We carefully examine a model system consisting of octane, water and carbon black. We use these results to guide our work on the emulsification of crude oil, a specific application studied here.

We use optical and cryogenic scanning electron microscopy to image emulsions. Their stability is monitored using centrifugation. Zeta potentials of the particles at different pH and salt concentrations provide key insights into the formation and stability of these emulsions. Since low molecular weight polycyclic aromatic hydrocarbons (PAH) in crude oil can partition into surrounding water, there is interest in finding methods to lower this transfer to reduce potential toxicity to marine organisms after an oil spill. In this context, we examine the adsorption of a model low molecular weight PAH, naphthalene, from the oil phase in an emulsion onto the CB

particles. As a potential application of these particles, we demonstrate the successful formation of stable crude oil (taken from the Gulf of Mexico Deepwater Horizon oil spill) -in-sea water emulsions. We compare the nature and lifetimes of Corexit 9500A stabilized emulsions with those stabilized by CB and show major differences between the two.

**2.3 Materials**

The para amino benzoic acid (PABA) terminated carbon black suspension in water at pH 7.5 is obtained from Cabot Corporation. PABA is covalently linked to the carbon surface, at a treatment level of 0.1-4.0 $\mu M/m^2$, adequate to make the particles hydrophilic and completely dispersible in water.[44] There are no surfactants in the CB suspension. N-octane (anhydrous, ≥99.0%), pyrene (puriss. p.a., for fluorescence, ≥99.0%), Aerosol OT (AOT, 99%) and 1N hydrochloric acid are obtained from Sigma Aldrich. Sodium chloride is obtained from Fisher Scientific. Crude Oil from the Gulf of Mexico oil spill, BP-MC 252 and Corexit 9500A are obtained through the Gulf of Mexico Research Initiative program. Corexit 9500A is a mixture of surfactants dissolved in polypropylene glycol. All materials are used as received.

**2.4 Methods**

**2.4.1** Preparation of emulsions

We use a 0.015wt% carbon black suspension for our experiments. Two routes are used to make the emulsions. In the first, 1N hydrochloric acid is added to the suspension to lower the pH to 3.3. The surface carboxylate groups get partially protonated, and the hydrophobicity of the particles increase. Emulsions are also formed by adding sodium chloride to the CB suspension. We use 0.6M NaCl to

roughly match the overall salt concentration in sea water (~3.5wt%); the $Na^+$ ions salt out some of the carboxylate groups on the surface of the CB. The protonation or the binding of sodium ions to the surface carboxylate groups results in increased particle hydrophobicity and chaining of the particles in the aqueous medium, producing a noticeable rise in the aqueous suspension viscosity. Rapid aggregation of the CB particles causes a difficulty in zeta potential measurements at 0.6M NaCl. To gain insights into the effects of salt addition through such measurements, we have used 0.15M NaCl suspensions for some of our experiments. In experiments with sea water, the emulsification proceeds without addition of any acid or salt to the CB suspension.

The acid- or salt- mediated CB suspensions are vortexed for 10 seconds at 3000 RPM. N-octane at an oil:water volumetric ratio of 3:5 is then added to the suspension and vortexed at 3000 RPM for 1 min, resulting in the emulsion. At these concentrations, most of the carbon black transfers from the aqueous phase to the oil-water interfaces of the freshly formed drops. This method of forming emulsions produces droplets of a wide size distribution, ranging from a few microns to a few hundred microns. Emulsions are also prepared using sea water and with crude oil BP-MC 252 as well as with Corexit 9500A and with AOT, one of the major components of Corexit 9500A. For the Corexit 9500A experiments, the surfactant is dissolved in the oil in a 1:20 surfactant solution to oil volumetric ratio. A 10mM AOT solution in crude oil is used for those experiments. For these latter two experiments, sea water is added to the oil containing surfactants. The CB suspension is then added, and the mixture vortexed for 1 min. at 3000RPM to form emulsions.

**2.4.2** Emulsion stability

When an oil-in-water emulsion is subjected to a centrifugal field, the denser aqueous phase collects at the end of the tube furthest from the axis of rotation, and the lighter emulsion-containing phase moves to the other end. During this process the oil droplets are forced against each other, and at a critical centrifugation rate, the first few drops start to coalesce. The pressure exerted on the oil droplets at these conditions is termed the critical de-emulsification pressure and is a reasonable measure of the stability of the emulsion under forced coalescence.[45] The critical de-emulsification pressure permits a quantitative comparison of the stability of emulsions formed under different conditions. If accelerations beyond the critical value are used, additional drop-drop coalescence take place, more oil is released, and a new equilibrium is established. The critical de-emulsification pressure, $P_{deemulsification}$ is calculated by measuring the volume of oil released at a particular centrifugal acceleration[46, 47] using [48]

$$P_{deemulsification} = \Delta\rho\, g_k\, (V_{oil} - V_{released})/A, \qquad (2)$$

where $\Delta\rho$ is density difference between the aqueous and oil phases, $g_k$ is the centrifugal acceleration, $V_{oil}$ is the total volume of oil in the emulsion, $V_{released}$ is volume of oil released after centrifugation, and A is the cross sectional area of the centrifuge tube.

Emulsions are centrifuged using an International Equipment Company (IEC) clinical centrifuge for 15 minutes. The centrifugal acceleration is varied between 150g and 1000g. After centrifugation, the released oil is withdrawn carefully from the top of the centrifuge tube with a syringe and its volume measured, from which the critical pressure for deemulsification is calculated using Eq. (2).

**2.4.3** Cryogenic Scanning Electron Microscopy (cryo-SEM)

Approximately 5µl of the emulsion is placed on a cylindrical sample holder. Both are then plunged into liquid nitrogen, rapidly solidifying the emulsion. The sample is fractured with a flat-edge cold knife at -130°C, then warmed to -95°C for a few minutes to sublime some of the residual octane and water. Sublimation enhances surface topological details. The sample is then cooled back to -130°C, sputtered with a gold-palladium composite, then moved from the preparation chamber to the imaging stage. A Hitachi S-4800 Field Emission SEM operated at 3kV and 20µA is used for imaging. The sample is maintained at -130°C during imaging. All of the processes starting from the fracturing to the imaging take place under a high vacuum.

**2.4.4** Additional characterization

**A** ZEISS Axioplan 2 Imaging System is used for fluorescence microscopy. A Nikon Eclipse E 600 and a Fisher Scientific Micromaster are used for brightfield optical microscopy. A Malvern Zetasizer is employed for zeta potential measurements. Samples for cryogenic transmission electron microscopy (cryo-TEM) are prepared in a controlled environment vitrification system manufactured at the Technion. The CB suspension is vortexed for 10 sec after addition of either acid or salt, transferred to a holey carbon TEM grid after 1 min and then vitrified in liquid ethane. Vitrified samples are transferred to a Gatan 626DH cryo holder maintained at -175**°C**, and imaged using a JEOL JEM 2100 Transmission Electron Microscope operating at 200kV.

**2.4.5** Napthalene adsorption

A 600ppm naphthalene solution is formed in octane, and used for forming the emulsion. The samples are allowed to stand for 72hrs at 25ºC (based on kinetic studies[49] adsorption equilibrium is established in this time frame). The emulsion is then destabilized by centrifuging at 5000g for 15min. A clear octane phase forms at the top, a clear aqueous phase forms at the bottom, and a thin layer of CB is sandwiched between these two phases. A small volume of octane is withdrawn from the top, diluted 30 times and then analyzed using **a** Shimadzu QP2010S GC-MS to determine naphthalene concentration. A control experiment without carbon black is also performed. In this case droplets form immediately upon vortexing, but separate into an oil phase and water phase as soon as the mixing stops. These samples are vortexed 5 times over a 72hr period, to ensure naphthalene transport away from the octane is complete, prior to measuring the concentration.

**2.5 Results and discussion**

Fig. 1 outlines the processes used to create the emulsions. A cryo-TEM image of a 0.015% w/w CB suspension is shown in Figure 1(a). Individual CB particles are observed, as is expected from a stable aqueous suspension of hydrophilic particles (the average interparticle distance is of the order of 2μm for this suspension, so we do not see more than one particle in these cryo-TEM images at the magnification needed to see one particle, but this is a typical image seen in various portions of the TEM grid). Upon the addition of HCl or NaCl, particles start agglomerating. Cryo-TEM images of such agglomerated particles are shown in Fig. 1(b) and Fig. 1(c). We do not observe

any unagglomerated particles in the acid or salt mediated cases, suggesting that

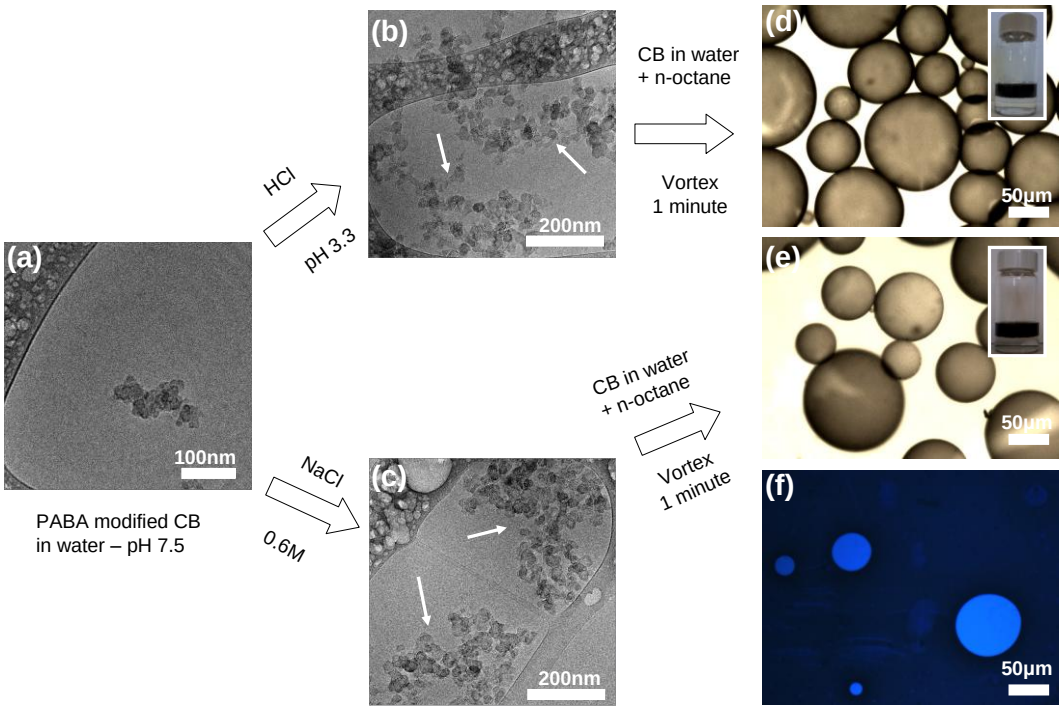


**Figure 1.** **(a)** Cryo TEM image showing a single carbon black (CB) particle of p-amino benzoic acid terminated, pH 7.5, 0.015% w/w suspension CB in water. Addition of HCl or NaCl make the particles partially hydrophobic and causes particle-particle agglomeration, shown by arrows in the cryo TEM images **(b)** and **(c)**. Addition of octane to the acid- or salt-mediated suspension followed by vortexing results in oil-in-water emulsions **(d)** and **(e)**. The oil droplets are in equilibrium with excess water that is free of carbon black as shown in the insets **(f)** fluorescence image of the acid-mediated sample with pyrene-labeled octane, confirming that this is an oil-in-water emulsion.

changing the CB surfaces from hydrophilic to partially hydrophobic drives agglomeration, and is consistent with an observed increase in suspension viscosity. Upon addition of octane and vortexing, shear induced in the system generates new oil-water interfaces, drives the CB into these interfaces and stabilizes the emulsion. The bottom aqueous phase looks clear and is in equilibrium with the top emulsion phase. Examination of this bottom phase by optical microscopy revealed a carbon black concentration that is about five orders of magnitude lower than that in the original suspension, suggesting that most of the CB is at the octane-water interfaces. Optical

micrographs of the emulsion droplets are shown in Fig. 1(d) and Fig. 1(e). A few drops of water disperse immediately when added to this emulsion, while drops of octane 'bead' up. When the octane is labeled with pyrene, and the emulsion imaged in fluorescence mode, the droplets are clearly visible (Fig. 1(f)). These experiments confirm that we have produced octane-in-water emulsions.

Cryo-SEM provides a more detailed insight into the structure of the particle aggregates and their positioning at the oil-water interfaces. Fig. 2(a) shows an image of an octane droplet in an emulsion prepared after addition of acid to a 0.015%w/w CB suspension. Multiple layers of CB consisting of closely packed particle aggregates are present at the interface, more evident in the higher magnification image of the interface in Fig. 2(b). The aggregation of particles upon addition of acid implies that the entities that reside at the oil-water interfaces are not individual carbon black particles but rather clusters of a few. We see evidence of these in our cryo-TEM images. Such clusters are harder to displace from oil-water interfaces than individual CB particles because the displacement energy scales with the square of the particle size, and provide additional stability for the emulsions. Emulsions have also been formed at 0.0075% w/w CB, shown in Fig. 2(c) and Fig. 2(d). We observe incomplete coverage of the droplet surface, but the emulsions are stable. We propose that the increased interfacial shear viscosity produced by the presence of a connected network of particles at the surface prevents thinning of the intervening water layer as droplets approach each other, and is responsible for suppressing coalescence. Fig. 2(e) and Fig. 2(f) show a typical CB-stabilized octane droplet from an emulsion prepared by addition of NaCl. While its features in these images show similarities to those formed

using addition of acid, there are significant differences related to the hydrophobic-hydrophilic balance of the particles that are explored next.

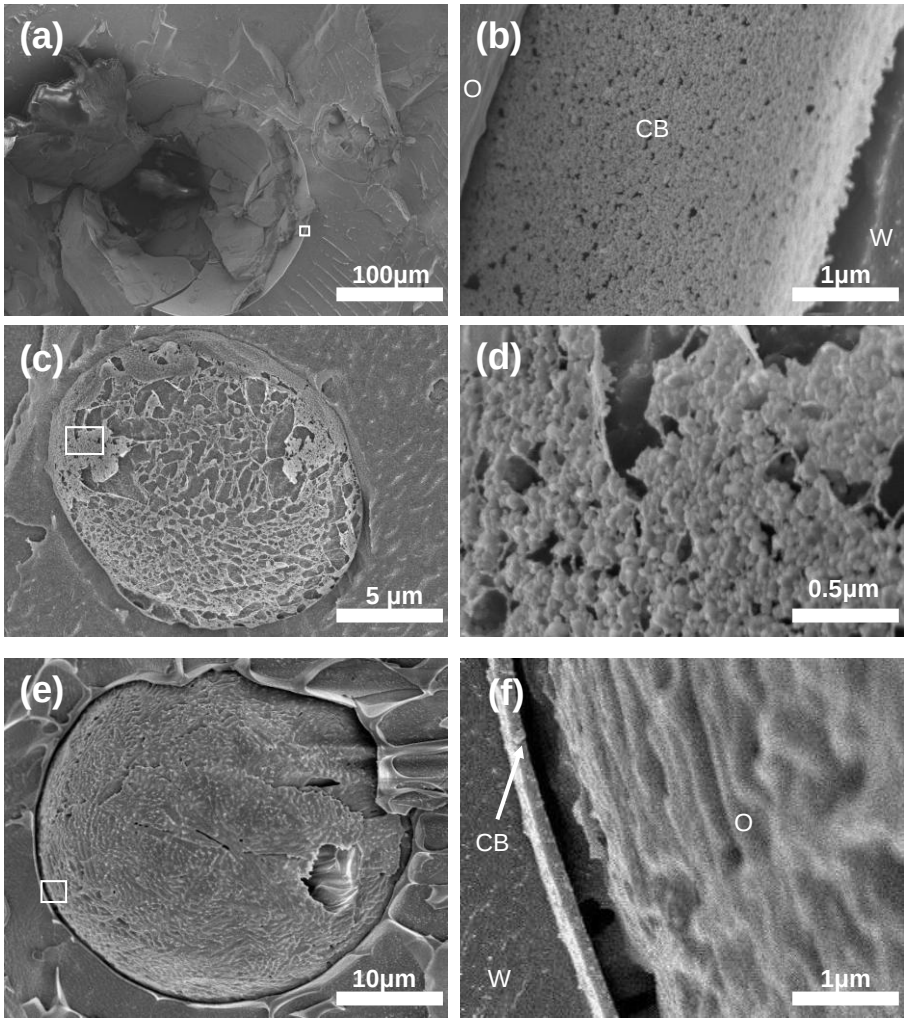


**Figure 2**: Cryo-SEM images of an octane-in water emulsion stabilized by carbon black at different conditions. **(a) (b)** pH 3.3, 0.015wt % CB; **(c) (d)** pH 3.3, 0.0075 wt% CB. At this CB concentration, the surface of the oil drop is not covered completely by particles. **(e) (f)** 0.6M NaCl, 0.015 wt% CB.

The coefficients of thermal expansion of octane and water are $0.001°C^{-1}$ and $0.0002°C^{-1}$ respectively.[50] During rapid sample solidification, the octane shrinks in volume more than the water, creating a gap at the octane-water interfaces. These gaps are a consequence of the cooling process, and they are often observed in rapidly solidified oil-in-water emulsions.[51, 52] Quite remarkably, for an emulsion prepared in

the presence of 0.15M NaCl, (Fig. 3(a) and Fig. 3(b)) the CB particles stay with the solidified aqueous phase. In contrast, for an emulsion prepared by the addition of acid, the particles stay with the octane (Fig. 3 (d) and Fig. 3(e)). If a major portion of the particle is within aqueous phase as it spans the oil-water interface, it stays with ice after freezing. Conversely, if most of the particle is in octane, it is pulled into the solidified octane upon freezing. Hydrophilic/hydrophobic balance of particles dictates particle location, and thus determines which phase they preferentially adhere to. To our knowledge, this is the first report of use of cryo-SEM to connect particle location to its hydrophilic/hydrophobic balance. Fig. 3(c) and Fig. 3(f) illustrate this concept.

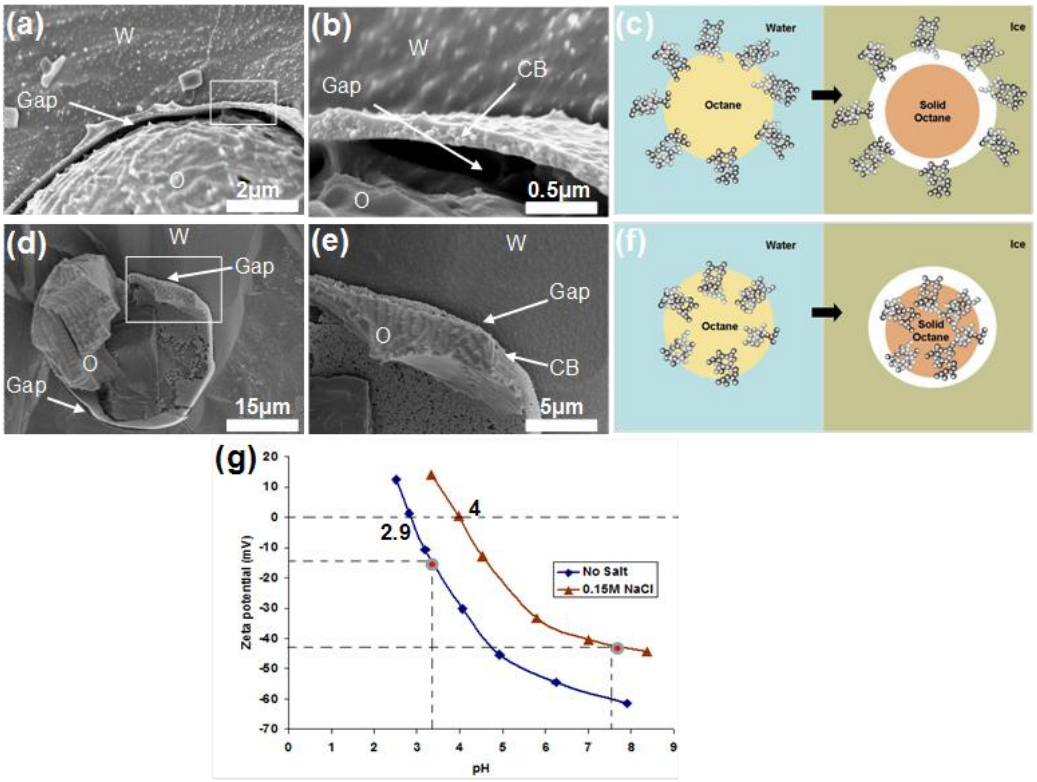


**Figure 3. (a) (b)** Cryo-SEM image of an octane-in-water emulsion stabilized by carbon black for pH 7.5, NaCl 0.15M, showing CB particles staying with aqueous phase **(c)** Model illustrating the location of most carbon black particles with the water phase **(d) (e)** Cryo-SEM image of a octane-in-water emulsion stabilized by carbon black at pH 3.3 showing CB staying with octane. **(f)** Model showing the location of most carbon black particles with the octane **(g)** Zeta potentials of CB particles suspended in water or a 0.15M NaCl solution. The red dot marked zeta potentials correspond to conditions used in the experiments.

Since many of the features observed in these emulsions are related to the hydrophilic/hydrophobic balance of the CB particles, which in turn are related to the residual charge on the particle surface, we measured zeta potentials for the particles under different conditions, and report them in Fig. 3(g). The zeta potential of the particles in the unmodified CB suspension is -60mV. When the pH is lowered to 3.3, the zeta potential is -15mV, indicating protonation of some surface carboxylate groups on the CB particles. At 0.15M NaCl, the zeta potential changes to -42mV, caused by salting of some carboxylate groups. The isoelectric point of the CB particles is 2.9 for no salt, shifts upward to 3.5 for 0.01M NaCl and 4.0 for 0.15M NaCl, indicating specific binding of sodium ions. The salt-modified particles carry substantially more charge than those modified by a change in pH, and are thus more hydrophilic. As further support, we note that the solubility of sodium benzoate in water is ~4M at 20°C while that of benzoic acid in water is 0.02M at 20°C.[53] These measurements are consistent with the observation that more hydrophilic particles stay with the aqueous phase upon freezing.

We compare the stability of the acid- and salt-mediated emulsions using centrifugation, and report results in Table 1. The key observation is that the salt-containing emulsions have a higher critical deemulsification pressure than those stabilized using the acid. The zeta potential measurements revealed that the salt-mediated particles have more charge than those formed by addition of acid, and are therefore more hydrophilic. We propose that these particles are able to bridge octane drops across an intervening water layer, and suppress drop-drop coalescence. We

show evidence of particle bridging in Fig. 4(a) and Fig. 4(b), and have observed many such particle-bridged drops in our salt-containing samples. Particle bridging is

**Table 1 – Critical de-emulsification pressure for different emulsions**

| Emulsion type | Critical deemulsification pressure |
|---|---|
| 0.6M NaCl<br>(0.015 wt% CB) | 4.6 kPa |
| pH 3.3<br>(0.015 wt% CB) | 2.2 kPa |
| 0.0075 wt% CB<br>(pH 3.3) | 1.4 kPa |

Critical deemulsification pressure for different emulsions. Repeated experiments show a variability of ~5% in the critical deemulsification pressure.

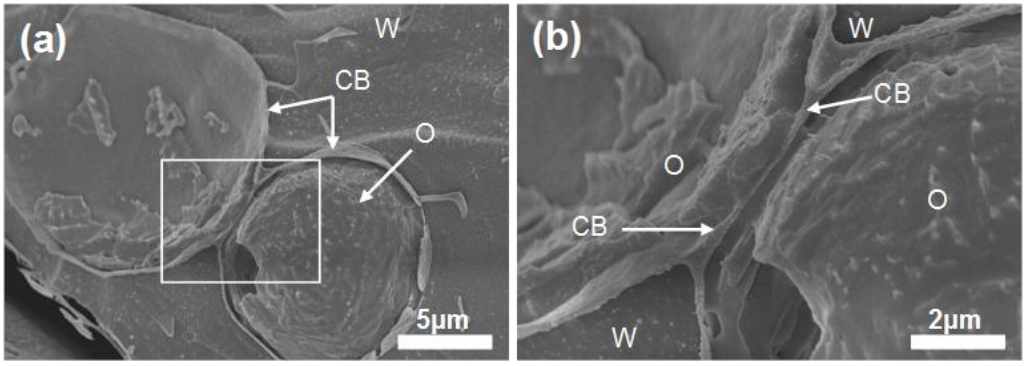


**Figure 4**: (a) (b) Two octane drops bridged by CB particles in a sample prepared using 0.015 wt% CB and 0.6M NaCl.

unlikely if the CB is too hydrophobic, and we have not observed any 'bridged' drops for the acid-mediated samples. If left unperturbed, both types of emulsions are stable against coalescence for months. The volume of the emulsion phase does not change over this time period.

Given the high specific surface area of CB particles, and non-specific binding capability of carbon, we have examined the absorption of naphthalene as a model polycyclic aromatic hydrocarbon from octane-in-water emulsions stabilized by CB on to the surface of the particles and report results in Table 2. The concentration of naphthalene in oil is reduced dramatically from the control case with no carbon black. More naphthalene is adsorbed for the acid-mediated case than the salt mediated emulsions as a consequence of the greater hydrophobicity of the acid-mediated emulsions.

**Table 2 – Napthalene adsorption**

| Experiment | Napthalene conc. in octane | Napthalene adsorbed (by mass) |
|---|---|---|
| pH 3.3, 0.015 wt% CB | 426 ppm | 27.7 % |
| pH 3.3, 0.0075 wt% CB | 567 ppm | 3.8% |
| 0.6 M NaCl, 0.015 wt% CB | 575 ppm | 2.4% |
| Control | 589 ppm | NA |

Napthalene adsorption under different conditions. The reduced concentration of naphthalene in octane compared to the control case indicates that the CB particles adsorb naphthalene from the octane. The last column is obtained by doing a mass balance for the naphthalene.

The successful formation of octane-in-water emulsions indicates that these particles have potential for use in crude oil emulsification in the event of a spill. To that end, we use crude oil from the Gulf of Mexico Oil Spill, BP-MC-252, to form emulsions. Fig. 5(a) shows emulsions formed with 10vol% oil using an acid-mediated CB suspension, while Fig. 5(b) shows an emulsion formed using a 0.6M NaCl mediated suspension. Both are crude-oil-in water single emulsions. They have been left in our laboratory for six months and have not shown any phase separation or changes to the volume of the emulsion phase over this time period.

Emulsions prepared by using 0.015 wt% CB, sea water from Narragansett Bay and 10 vol% crude oil result in crude oil-in-water emulsions, shown in Fig. 5(c) and Fig. 5(d). While we show an image taken after one hour, this emulsion stays stable in a vial for several months. As a comparison, we use Corexit 9500A to form an emulsion with 10 vol% crude oil and 90 vol% sea water. An optical micrograph of the resulting emulsion, taken right after vortexing, is shown in Fig. 5(e). These are water-in-crude oil-in-water double emulsions. This double emulsion destabilizes in about an hour in a vial. Interestingly, the 'top' phase at this point consists of a layer of oil with water drops dispersed within it, or a water-in-oil emulsion, shown in Fig. 5(f). This is a key difference between the CB- and Corexit 9500A- stabilized crude oil/sea water emulsions.

Crude oil contains asphaltenes and resins.[10, 54, 55 56] We propose that the interaction of these components with Corexit 9500A[57, 58] promotes the formation of water-in-crude-oil-in-water double emulsions when first mixed. The double emulsion then

destabilizes rapidly to form the water-in-oil emulsion. We confirm this using a series

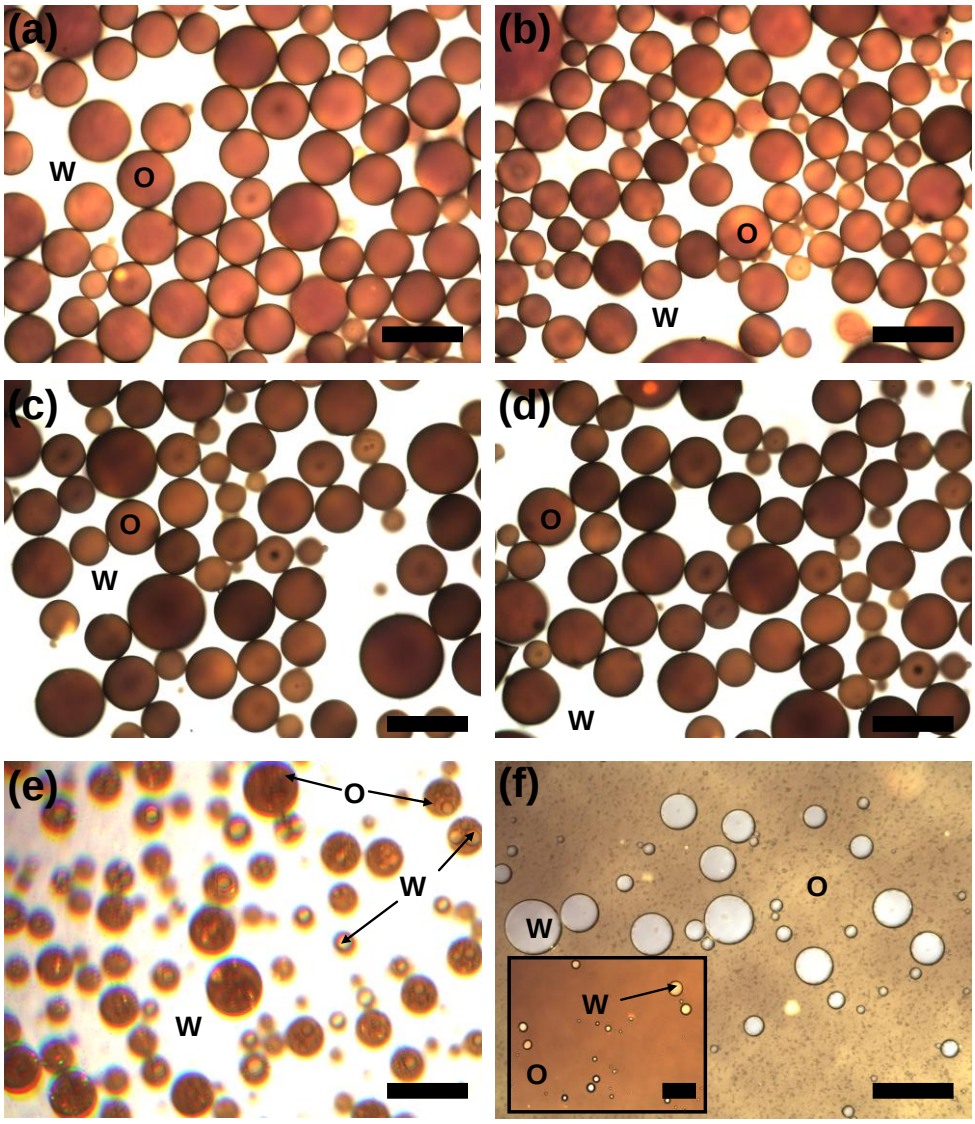


**Figure 5**: Oil-in water emulsions formed with 10 vol% BP-MC 252 crude oil, 0.015 wt% CB and DI water . Optical micrographs showing oil droplets in water for **(a)** pH 3.3 **(b)** 0.6M NaCl (W-water, O-oil) Optical micrographs of a 0.015 wt% CB in sea water mixed with BP-MC 252 crude oil, resulting in an oil – in water emulsion - **(c)** image taken immediately after mixing, **(d)** image taken1 hr after mixing, showing stable crude oil droplets in sea water. **(e)** Vortexing BP-MC 252 crude oil (10 vol%) containing Corexit 9500A (1:20 dispersant to oil ratio) with sea water (Narragansett bay) results in a water-in-oil-in-water (W/O/W) double emulsion. **(f)**The double emulsion in **(e)** transforms within an hour to a film of oil containing water drops, in equilibrium with water below. The inset in **(f)** shows a water- in-crude oil emulsion formed using 10mM AOT. Scale bars are 200 microns.

of experiments. First, when octane with Corexit 9500A is vortexed with sea water, no emulsion is produced. When crude oil without any added surfactant is vortexed with sea water, the emulsion is unstable, and the oil separates from the water; but we observe a few water drops dispersed within oil. When AOT, a major component of Corexit 9500A[59] is added to octane and vortexed with sea water, an emulsion is not produced. However, when AOT is added to the crude oil and the solution vortexed with sea water, a water-in-oil emulsion results, shown in the inset in Fig. 5(f). These results support our hypothesis that components of crude oil and Corexit 9500A interact to form water-in-oil emulsions. We note that for an oil spill remediation application, the presence of water droplets in the crude oil is undesirable because of the reduced calorific content, decreased ability to burn the oil, the reduction in bioremediation efficiency, the additional volume for removal,[56] and the increased viscosity.[56, 60]

Our experiments provide strong evidence that this CB suspension has potential for use as an alternative dispersant for subsurface oil spills. The detailed examination of octane-in-water emulsions and the successful formation of these emulsions with added NaCl provided key insights into the conditions necessary to form crude oil-in-sea water emulsions. The principle of *in situ* tuning of surface properties of particles to enhance their ability to form emulsions, in combination with the ability to exploit intrinsic particle properties, is a powerful strategy for making advanced materials that is being explored in our laboratory and elsewhere.

## 2.6 Conclusions

We demonstrate the formation of octane-in-water emulsions using carboxyl terminated carbon black particles. These emulsions are prepared either by dropping the pH, which makes the particles more hydrophobic by protonating surface carboxylate groups, or by adding NaCl, which imparts hydrophobicity due to specific adsorption and binding of the sodium ions to the particles. These two routes vary the hydrophilic/hydrophobic balance on the carbon black particles in different ways and by different amounts. We use cryo-SEM to characterize these emulsions, and examine particle configurations at the oil-water interfaces. The difference in thermal expansion coefficients for octane and water creates gaps between the oil and water phases upon rapid cooling and solidification, and provide insights into the hydrophobic/hydrophilic balance of the particles. The acid-modified particles are anchored deeply in the octane. Conversely, the more hydrophilic particles mediated by salt stay with the aqueous phase upon solidification. The critical de-emulsification pressure is higher for the salt-mediated particles than those where acid is added. Particle bridging in these salt-mediated emulsions is responsible for greater stability. We show evidence of significant adsorption of a model cyclic hydrocarbon, naphthalene, on to the surface of the CB particles. The formation of stable crude oil-in-sea water emulsions using these CB particles, without any supplementary acid or salt addition, has been demonstrated. In contrast, we observe unstable water-in-crude oil-in-water double emulsions when we use a commercial surfactant Corexit 9500A. Our study has broad implications for the development of particle-based dispersants that have specific application for emulsifying oil and keeping them stable in water columns in the event of an oil spill.

The strategy of tuning surface properties of particles prior to forming emulsions has applications in the synthesis of materials with novel combinations of properties.

## 2.7 Acknowledgements

We gratefully acknowledge the financial support provided by the National Science Foundation (CBET 0854115, 1043163, 1049330), the Rhode Island Consortium for Nanoscience and Nanotechnology, the Gulf of Mexico Research Initiative, Cabot Corporation and the University of Rhode Island Graduate Fellowship Program.

## References

1. Rico-Martinez, R.; Snell Terry, W.; Shearer Tonya, L., Synergistic toxicity of Macondo crude oil and dispersant Corexit 9500A(Â®) to the Brachionus plicatilis species complex (Rotifera). *Environmental pollution (Barking, Essex : 1987)* **2012,** 173C, 5-10.

2. Ramsden, W., The separation of solid materials on the surface of solutions and suspensions. Observations concerning surface diaphragms, foam blisters, emulsions and mechanical coagulation. [machine translation]. *Proceedings of the Royal Society of London* **1903,** 72, 156-64.

3. Pickering, S. U., Emulsions. *Journal of the Chemical Society, Transactions* **1907,** 91, 2001-21.

4. Finkle, P.; Draper, H. D.; Hildebrand, J. H., The theory of emulsification. *Journal of the American Chemical Society* **1923,** 45, 2780-8.

5. Schulman, J. H.; Leja, J., Control of contact angles at the oil-water-solid interfaces. Emulsions stabilized by solid particles (barium sulfate). *Transactions of the Faraday Society* **1954,** 50, 598-605.

6. Briggs, T. R., Emulsions with finely divided solids. *Journal of Industrial and Engineering Chemistry (Washington, D. C.)* **1921,** 13, 1008-10.

7. Frelichowska, J.; Bolzinger, M.-A.; Pelletier, J.; Valour, J.-P.; Chevalier, Y., Topical delivery of lipophilic drugs from o/w Pickering emulsions. *International Journal of Pharmaceutics* **2009,** 371, (1-2), 56-63.

8. Velev, O. D.; Furusawa, K.; Nagayama, K., Assembly of Latex Particles by using Emulsion Droplets as Templates. 1. Microstructured Hollow Spheres. *Langmuir* **1996,** 12, (10), 2374-84.

9. Hong, L.; Jiang, S.; Granick, S., Simple Method to Produce Janus Colloidal Particles in Large Quantity. *Langmuir* **2006,** 22, (23), 9495-9499.

10. Sullivan, A. P.; Kilpatrick, P. K., The Effects of Inorganic Solid Particles on Water and Crude Oil Emulsion Stability. *Industrial & Engineering Chemistry Research* **2002,** 41, (14), 3389-3404.

11. Lee, M. N.; Chan, H. K.; Mohraz, A., Characteristics of Pickering Emulsion Gels Formed by Droplet Bridging. *Langmuir* 28, (6), 3085-3091.

12. Rousseau, D., Fat crystals and emulsion stability - a review. *Food Research International* **2000,** 33, (1), 3-14.

13. Tambe, D. E.; Sharma, M. M., The effect of colloidal particles on fluid-fluid interfacial properties and emulsion stability. *Advances in Colloid and Interface Science* **1994,** 52, 1-65.

14. Moore, W. C., Emulsification of water and of ammonium chloride solutions (in kerosene) by means of lamp black. *Journal of the American Chemical Society* **1919,** 41, 940-6.

15. Tsugita, A.; Takemoto, S.; Mori, K.; Yoneya, T.; Otani, Y., Studies on O/W emulsions stabilized with insoluble montmorillonite-organic complexes. *Journal of Colloid and Interface Science* **1983,** 95, (2), 551-60.

16. Gelot, A.; Friesen, W.; Hamza, H. A., Emulsification of oil and water in the presence of finely divided solids and surface-active agents. *Colloids and Surfaces* **1984,** 12, (3-4), 271-303.

17. Hassander, H.; Johansson, B.; Toernell, B., The mechanism of emulsion stabilization by small silica (Ludox) particles. *Colloids and Surfaces* **1989,** 40, (1-2), 93-105.

18. Tamb, D. E.; Sharma, M. M., Factors controlling the stability of colloid-stabilized emulsions. I. An experimental investigation. *Journal of Colloid and Interface Science* **1993,** 157, (1), 244-53.

19. Abend, S.; Bonnke, N.; Gutschner, U.; Lagaly, G., Stabilization of emulsions by heterocoagulation of clay minerals and layered double hydroxides. *Colloid and Polymer Science* **1998,** 276, (8), 730-737.

20. Midmore, B. R., Preparation of a novel silica-stabilized oil/water emulsion. *Colloids and Surfaces, A: Physicochemical and Engineering Aspects* **1998,** 132, (2-3), 257-265.

21. Kim, J.; Cote, L. J.; Kim, F.; Yuan, W.; Shull, K. R.; Huang, J., Graphene Oxide Sheets at Interfaces. *Journal of the American Chemical Society* 132, (23), 8180-8186.

22. Dinsmore, A. D.; Hsu, M. F.; Nikolaides, M. G.; Marquez, M.; Bausch, A. R.; Weitz, D. A., Colloidosomes: Selectively Permeable Capsules Composed of Colloidal Particles. *Science (Washington, DC, United States)* **2002,** 298, (5595), 1006-1009.

23. Kaz, D. M.; McGorty, R.; Mani, M.; Brenner, M. P.; Manoharan, V. N., Physical ageing of the contact line on colloidal particles at liquid interfaces. *Nature Materials* 11, (2), 138-142.

24. McGorty, R.; Fung, J.; Kaz, D.; Manoharan, V. N., Colloidal self-assembly at an interface. *Materials Today (Oxford, United Kingdom)* 13, (6), 34-42.

25. Vignati, E.; Piazza, R.; Lockhart, T. P., Pickering Emulsions: Interfacial Tension, Colloidal Layer Morphology, and Trapped-Particle Motion. *Langmuir* **2003,** 19, (17), 6650-6656.

26. Ashby, N. P.; Binks, B. P.; Paunov, V. N., Bridging interaction between a water drop stabilized by solid particles and a planar oil/water interface. *Chemical Communications (Cambridge, United Kingdom)* **2004**, (4), 436-437.

27. Horozov, T. S.; Aveyard, R.; Clint, J. H.; Neumann, B., Particle Zips: Vertical Emulsion Films with Particle Monolayers at Their Surfaces. *Langmuir* **2005,** 21, (6), 2330-2341.

28. Horozov, T. S.; Binks, B. P., Particle-stabilized emulsions: a bilayer or a bridging monolayer? *Angewandte Chemie, International Edition* **2006,** 45, (5), 773-776.

29. Binks, B. P., Particles as surfactants - similarities and differences. *Current Opinion in Colloid & Interface Science* **2002,** 7, (1,2), 21-41.

30. Nushtayeva, A. V.; Kruglyakov, P. M., Capillary pressure in a thinning emulsion film stabilised by spherical solid particles. *Mendeleev Communications* **2001**, (6), 235-237.

31. Kruglyakov, P. M.; Nushtayeva, A. V.; Vilkova, N. G., Experimental investigation of capillary pressure influence on breaking of emulsions stabilized by solid particles. *Journal of Colloid and Interface Science* **2004,** 276, (2), 465-474.

32. Reincke, F.; Kegel, W. K.; Zhang, H.; Nolte, M.; Wang, D.; Vanmaekelbergh, D.; Moehwald, H., Understanding the self-assembly of charged nanoparticles at the water/oil interface. *Physical Chemistry Chemical Physics* **2006,** 8, (33), 3828-3835.

33. Reincke, F.; Hickey, S. G.; Kegel, W. K.; Vanmaekelbergh, D., Spontaneous assembly of a monolayer of charged gold nanocrystals at the water/oil interface. *Angewandte Chemie, International Edition* **2004,** 43, (4), 458-462.

34. Larson-Smith, K.; Jackson, A.; Pozzo, D. C., SANS and SAXS Analysis of Charged Nanoparticle Adsorption at Oil-Water Interfaces. *Langmuir* 28, (5), 2493-2501.

35. Amalvy, J. I.; Armes, S. P.; Binks, B. P.; Rodrigues, J. A.; Unali, G. F., Use of sterically-stabilised polystyrene latex particles as a pH-responsive particulate emulsifier to prepare surfactant-free oil-in-water emulsions. *Chemical Communications (Cambridge, United Kingdom)* **2003**, (15), 1826-1827.

36. Aveyard, R.; Binks, B. P.; Clint, J. H., Emulsions stabilised solely by colloidal particles. *Advances in Colloid and Interface Science* **2003,** 100-102, 503-546.

37. Tarimala, S.; Dai, L. L., Structure of Microparticles in Solid-Stabilized Emulsions. *Langmuir* **2004,** 20, (9), 3492-3494.

38. Yan, N.; Gray, M. R.; Masliyah, J. H., On water-in-oil emulsions stabilized by fine solids. *Colloids and Surfaces, A: Physicochemical and Engineering Aspects* **2001,** 193, (1-3), 97-107.

39. Madivala, B.; Vandebril, S.; Fransaer, J.; Vermant, J., Exploiting particle shape in solid stabilized emulsions. *Soft Matter* **2009,** 5, (8), 1717-1727.

40. Ghezzi, F.; Earnshaw, J. C.; Finnis, M.; McCluney, M., Pattern Formation in Colloidal Monolayers at the Air-Water Interface. *Journal of Colloid and Interface Science* **2001,** 238, (2), 433-446.

41. Horozov, T. S.; Aveyard, R.; Clint, J. H.; Binks, B. P., Order-Disorder Transition in Monolayers of Modified Monodisperse Silica Particles at the Octane-Water Interface. *Langmuir* **2003,** 19, (7), 2822-2829.

42. Casado, R. M.; Lovell, P. A.; Navabpour, P.; Stanford, J. L., Polymer encapsulation of surface-modified carbon blacks using surfactant-free emulsion polymerization. *Polymer* **2007,** 48, (9), 2554-2563.

43. Sharif Sh, M.; Golestani Fard, F.; Khatibi, E.; Sarpoolaky, H., Dispersion and stability of carbon black nanoparticles, studied by ultraviolet-visible spectroscopy. *Journal of the Taiwan Institute of Chemical Engineers* **2009,** 40, (5), 524-527.

44. Johnson, J. E.; Belmont, J. A. Modified colored pigments and ink jet inks, inks, and coatings containing modified colored pigments. 1997-871453 5922118, 19970609., 1999.

45. San-Miguel, A.; Behrens, S. H., Influence of nanoscale particle roughness on the stability of pickering emulsions. *Langmuir* 28, (33), 12038-12043.

46. Princen, H. M., Osmotic pressure of foams and highly concentrated emulsions. I. Theoretical considerations. *Langmuir* **1986,** 2, (4), 519-24.

47. Princen, H. M.; Kiss, A. D., Osmotic pressure of foams and highly concentrated emulsions. 2. Determination from the variation in volume fraction with height in an equilibrated column. *Langmuir* **1987,** 3, (1), 36-41.

48. Tcholakova, S.; Denkov, N. D.; Ivanov, I. B.; Campbell, B., Coalescence in Î²-Lactoglobulin-Stabilized Emulsions: Effects of Protein Adsorption and Drop Size. *Langmuir* **2002,** 18, (23), 8960-8971.

49. Ania, C. O.; Cabal, B.; Pevida, C.; Arenillas, A.; Parra, J. B.; Rubiera, F.; Pis, J. J., Effects of activated carbon properties on the adsorption of naphthalene from aqueous solutions. *Applied Surface Science* **2007,** 253, (13), 5741-5746.

50. Green, D., Perry, R., *Perry's Chemical Engineers' Handbook*. Mc-Graw Hill: New York.

51. Jahaniaval, F.; Kakuda, Y.; Abraham, V., Characterization of a double emulsion system (oil-in-water-in-oil emulsion) with low solid fats: Microstructure. *Journal of the American Oil Chemists' Society* **2003,** 80, (1), 25-31.

52. Binks, B. P.; Rodrigues, J. A., Influence of surfactant structure on the double inversion of emulsions in the presence of nanoparticles. *Colloids and Surfaces, A: Physicochemical and Engineering Aspects* **2009,** 345, (1-3), 195-201.

53. Wibbertmann, A.; Kielhorn, J.; Koennecker, G.; Mangelsdorf, I.; Melber, C., Concise international chemical assessment document 26. Benzoic acid and sodium

benzoate. *Concise International Chemical Assessment Document* **2000**, (26), i-iv, 1-48.

54. Sjoblom, J.; Urdahl, O.; Hoeiland, H.; Christy, A. A.; Johansen, E. J., Water-in-crude oil emulsions. Formation, characterization, and destabilization. *Progress in Colloid & Polymer Science* **1990,** 82, (Surfactants Macromol.: Self-Assem. Interfaces Bulk), 131-9.

55. Mackay, G. D. M.; McLean, A. Y.; Betancourt, O. J.; Johnson, B. D., Formation of water-in-oil emulsions subsequent to an oil spill. *Journal of the Institute of Petroleum* **1973,** 59, (568), 164-72.

56. *Emulsion and Emulsion Stability*. Second ed.; Taylor & Francis Group: New York, 2005; Vol. Surfactant Science Series Volume 132.

57. Salmon-Vega, S.; Herrera-Urbina, R.; Valdez, M. A.; Lira-Galeana, C., Effect of the concentration of ionic surfactants on the electrokinetic behavior of asphaltene precipitated from a Maya Mexican crude oil. *Revista Mexicana de Ingenieria Quimica* 9, (3), 343-357.

58. Hashmi, S. M.; Firoozabadi, A., Tuning size and electrostatics in non-polar colloidal asphaltene suspensions by polymeric adsorption. *Soft Matter* 7, (18), 8384-8391.

59. *Oil Spill Dispersants: Efficacy and Effects*. The National Academies Press: 2005.

60. Cormack, D., *Response to marine oil pollution – review and assessment*. Springer: Dordrecht, 1999.

# CHAPTER 3

## In situ Assembly of Hydrophilic and Hydrophobic Nanoparticles at Oil-Water Interfaces as a Versatile Strategy to form Stable Emulsions

(under review in ACS Nano)

Amitesh Saha,[†] Vijay T. John,[‡] Arijit Bose[†*]

† Department of Chemical Engineering, University of Rhode Island, Kingston, RI 02881, USA

‡Department of Chemical and Biomolecular Engineering, Tulane University, New Orleans, LA 70118, USA.

*Corresponding author: Arijit Bose; tel: 401-874-2804, email: bosea@egr.uri.edu

## 3.1 Abstract

We report a conceptually new strategy for forming particle-stabilized emulsions. We begin with stable, dilute suspensions of highly hydrophilic nanoparticles in water and hydrophobic nanoparticles in oil. When the two suspensions are mixed, attractive van der Waals interactions between the hydrophilic and hydrophobic particles cause them to assemble at the oil-water interfaces into supraparticle aggregates that are partially wettable in both phases. These aggregates effectively stabilize emulsions. Both water-in-oil as well as oil-in-water emulsions can be formed by tuning the ratio of hydrophilic to hydrophobic particles in aggregates. Because each of the particle suspensions are stable and unaggregated, this method of forming emulsions requires less energy/volume compared to ones formed from single, partially wettable particles. When the Hamaker constants of aqueous and oil phases are chosen to be intermediate between the Hamaker constants of the two types of particles, repulsive interactions between these particles prevent the formation of partially wettable aggregates, and emulsions are not formed. Van der Waals interaction energy between two particle types across an aqueous-organic interface provide a systematic guide to particle and liquid combinations that can be used for stabilizing emulsions using our strategy. Our analysis and experiments provide a new platform for the formation of particle-stabilized emulsions and can be used to combine particles of different functionalities at emulsion droplet surfaces for generating novel materials.

## 3.2 Introduction

Emulsions stabilized solely by particles were first reported over 100 years ago by Ramsden[1] and by Pickering[2]. These emulsions require particles to locate at liquid-

liquid interfaces. This process can be understood by examining the energy of detachment, $\Delta E$, for a model spherical particle from a liquid-liquid interface into either bulk phase, and is given by

$$\Delta E = \pi R^2 \gamma_{ow} (1 - |\text{Cos } \theta|)^2. \qquad (1)$$

Here R is the particle radius, $\gamma_{ow}$ is the oil-water interfacial tension and $\theta$ is the contact angle through either phase. For a typical oil-water interfacial tension of 35mN/m and R = 10nm, $\Delta E > 500$ kT for $55^o < \theta < 125^o$. Particles with these contact angles are partially wettable in both phases, and would hence lodge preferentially and irreversibly at oil-water interfaces, helping to stabilize emulsion droplets.[3, 4] One consequence of this partial wettability is that these particles will have a tendency to agglomerate or form a network in the phase they are suspended in, to minimize the overall free energy. Individual nanoparticles can stay suspended because their Brownian motion dominates over sedimentation. However agglomeration often causes the particles to sediment, while network formation results in a large increase of the zero shear viscosity. [5, 6] Thus, creating a homogeneous dispersion of individual partially wettable particles requires a sustained input of energy up to the time a second immiscible liquid is added to form an emulsion. In this paper, we describe a conceptually new process for creating a particle-stabilized emulsion that relies on the *in situ* assembly of fully wettable particles at liquid-liquid interfaces to create partially wettable aggregates that can stabilize emulsions. This process can be applied to a broad range of particles, opening up the possibility of making emulsions and materials that have unique functionalities.

We begin with stable suspensions of highly hydrophilic particles in water and highly hydrophobic particles in oil. When these two dispersions are mixed, the hydrophilic and hydrophobic particles 'bind' at the oil-water interfaces through attractive van der Waals interactions with energies that are multiples of kT, and form partially wettable supraparticle complexes. These complexes then stabilize emulsion droplets. We perform energy calculations to guide choices of particles and liquids that will successfully form emulsions using this approach.

### 3.3 Materials

Dimethyldichlorosilane treated hydrophobic fumed silica was obtained from Cabot Corporation. These particles have a fractal structure of nominal size ~ 100nm with primary particles having a diameter of ~ 10nm.. Spherical silica particles (~80nm), surface modified with methacrylate silane to make them hydrophobic, were obtained from Nyacol Corporation. A para amino benzoic acid (PABA) terminated carbon black suspension in water at pH 7.5 was obtained from Cabot Corporation. PABA is covalently linked to the carbon surface, at a treatment level of 0.1-4.0 $\mu M/m^2$, adequate to make the particles hydrophilic and completely dispersible in water.[20] The nominal diameter of these fractal particles is about 120nm with ~20nm diameter primary particles. Hydrophilic spherical iron oxide particles (~10nm) were obtained from Ferro Tec. Anhydrous toluene of purity ≥99.0% and p-xylene of 99+% purity were obtained Sigma Aldrich. Polyethylene glycol 200 was obtained from Alfa Aesar. The Hamaker constants, A, of these materials are $A_{carbon\ black} = 4.7x10^{-19}J$, [13, 21] $A_{iron\ oxide} = 2.1\ x10^{-19}J$,[13] $A_{silica} = 6.2x10^{-20}J$,[22] $A_{toluene} = 5.4x10^{-20}J$,[22] $A_{water} = 3.7x10^{-20}J$,[13, 22] $A_{PEG} = 7.5x10^{-20}J$, [22] and $A_{p\text{-}xylene} = 7.0x10^{-20}J$.[13]

## 3.4 Methods

### 3.4.1 Preparation of Emulsions

Carbon black suspensions at 0.015wt%, and a 0.015 wt% hydrophilic iron oxide suspension are prepared in deionized water. The hydrophobic fumed silica and spherical silica particles are dispersed in toluene to form a 0.015 wt% suspension. Different volume ratios of these suspensions are vortexed at 1200 RPM for 1 minute to form toluene–in-water or water-in-toluene emulsions.

### 3.4.2 Microscopy

A Gatan Alto 2500 sample preparation system, along with a Zeiss Sigma VP FESEM is used for cryogenic scanning electron microscopy. A Nikon Eclipse E 600 is used for brightfield optical microscopy.

## 3.5 Results and Discussion

We first establish the framework for the selection of particles and liquids for our experiments. The two major components to particle movement across an oil-water interface come from van der Waals forces between particles, and electrostatic interactions between a charged particle and a charged oil-water interface.[8-12] Using material properties that are representative of our system and at a separation distance of 0.1nm, the van der Waals contribution is ~ -30 kT, while the electrostatic contribution is 0.03kT. Hence electrostatic repulsion can be safely ignored.

Following previous work,[13-17] we obtain an expression for the van der Waals energy of interaction between two particles through two immiscible liquids. As the distance between particles becomes small compared to the particle dimensions, we ignore the particle curvature, and model the system as two semi-infinite flat plates interacting

across two immiscible liquids, shown in Fig. 1(a). The van der Waals energy U, of a particle P1 in a medium M1 interacting with a particle P2 in medium M2 across a M1-M2 interface is given by:

$$-U = \frac{1}{12\pi(\Phi d)^2}\left(A_{P1}^{\frac{1}{2}} - A_{M1}^{\frac{1}{2}}\right)\left(A_{M2}^{\frac{1}{2}} - A_{M1}^{\frac{1}{2}}\right) + \frac{1}{12\pi(1-\Phi)^2 d^2}\left(A_{P2}^{\frac{1}{2}} - A_{M2}^{\frac{1}{2}}\right)\left(A_{M1}^{\frac{1}{2}} - A_{M2}^{\frac{1}{2}}\right) + \frac{1}{12\pi d^2}\left(A_{P1}^{\frac{1}{2}} - A_{M1}^{\frac{1}{2}}\right)\left(A_{P2}^{\frac{1}{2}} - A_{M2}^{\frac{1}{2}}\right) \quad (2)$$

$A_i$ is the Hamaker constant of material 'i', d is the distance between two particles and $\phi$ is the fraction of the distance d occupied by M1. U < 0 implies attractive interactions between P1 and P2, while U > 0 implies repulsive interactions. In our experiments, P1 is chosen to be either hydrophilically modified carbon black or iron oxide, while P2 is hydrophobically modified silica. We chose water as M1 and toluene as M2. Toluene is selected for these experiments because it has a Hamaker constant in the higher range for oils, and can dissolve p-xylene, a high Hamaker constant solute. We note that the surface modification on each type of particle will modulate the interparticle interaction energy, but that effect is small compared to the energy of interaction between P1 and P2. We show lines of U=0 at $\phi$=0, corresponding to only toluene as medium, $\phi$=1, corresponding to only water as medium, and $\phi$=0.5 in Fig. 1(a), and indicate the range of particle Hamaker constants where P1 and P2 will undergo either attractive or repulsive interactions. We hypothesize that emulsions can only be formed if the hydrophobic and hydrophilic particles interact attractively across oil-water interfaces, so that they assemble into partially wettable aggregates. As a general rule of thumb, this will happen if both

media between the particles have Hamaker constants that are either above or below that of P1 and P2. We identify points on this plot that correspond to the properties of the particles and liquids we have used. They are all in the regions where the interparticle interaction is attractive. Such particle liquid combinations should produce emulsions.

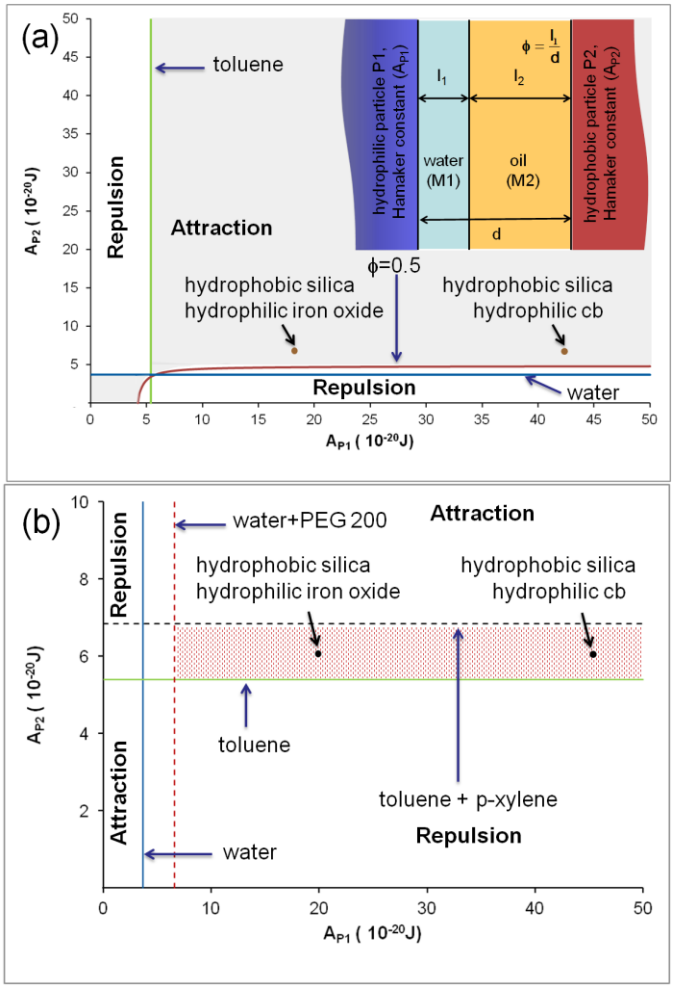


**Figure 1.** Range of Hamaker constants of particles that will show attractive and repulsive interactions across water-toluene interfaces. **(a)** U=0 for only water as the medium, only toluene as the medium and for $\phi$=0.5. The Hamaker constants of the particles are shown. These particles will interact attractively across the water-toluene interfaces. **(b)** U=0 for water, toluene, water + 80%w/w PEG 200 and toluene + 90%w/w p-xylene as the two immiscible media ($\phi$=0, $\phi$=1). When particle Hamaker constants are in the shaded region, the interparticle interactions go from being attractive to repulsive upon adding PEG 200 and p-xylene to water and toluene respectively.

If the Hamaker constants of the water and oil phases are intermediate between $A_{P1}$ and $A_{P2}$, the particles would interact repulsively. In Fig. 1(b) we show the consequence of making the aqueous phase to be 80% w/w PEG 200, and the toluene phase 90% w/w p-xylene, [18] raising the Hamaker constants of the aqueous and oil phases to above that of silica, but below that of carbon or iron oxide. Our particles now lie in a region where the interparticle interactions are repulsive. We propose that such particle-liquid combinations will not allow emulsions to form.

Some control experiments are performed first. Toluene is mixed into the aqueous hydrophilic particle suspension or water is mixed into the toluene suspension with hydrophobic particles. Te aqueous and organic phases separate fully and emulsions are not formed in either case.

When the CB suspension in water is mixed with the suspension of hydrophobic fumed silica in toluene, a stable emulsion is formed. Fig. 2(a) shows the assembly route for hydrophilic and hydrophobic particles at oil-water interfaces to form partially wettable entities that can stabilize an emulsion. The average wettability of the particle aggregate will determine whether an oil-in-water or a water-in-oil emulsion is formed. For a given set of particles, this can be controlled by varying the proportion of hydrophobic to hydrophilic entities in an aggregate. If the particle concentration in each of the suspensions is fixed, the volume ratio of the suspensions directly impacts the hydrophobic / hydrophilic balance of the supraparticle aggregates. Fig. 2(b) shows optical micrographs of a water-in-toluene emulsion formed by mixing a 0.015%w/w CB suspension in water with a 0.015%w/w fumed silica suspension in toluene at a ratio of 30:70 v/v. When this proportion is changed to 70:30 a toluene-in-water

emulsion is formed (Fig. 2(c)). To demonstrate the versatility of this technique, we

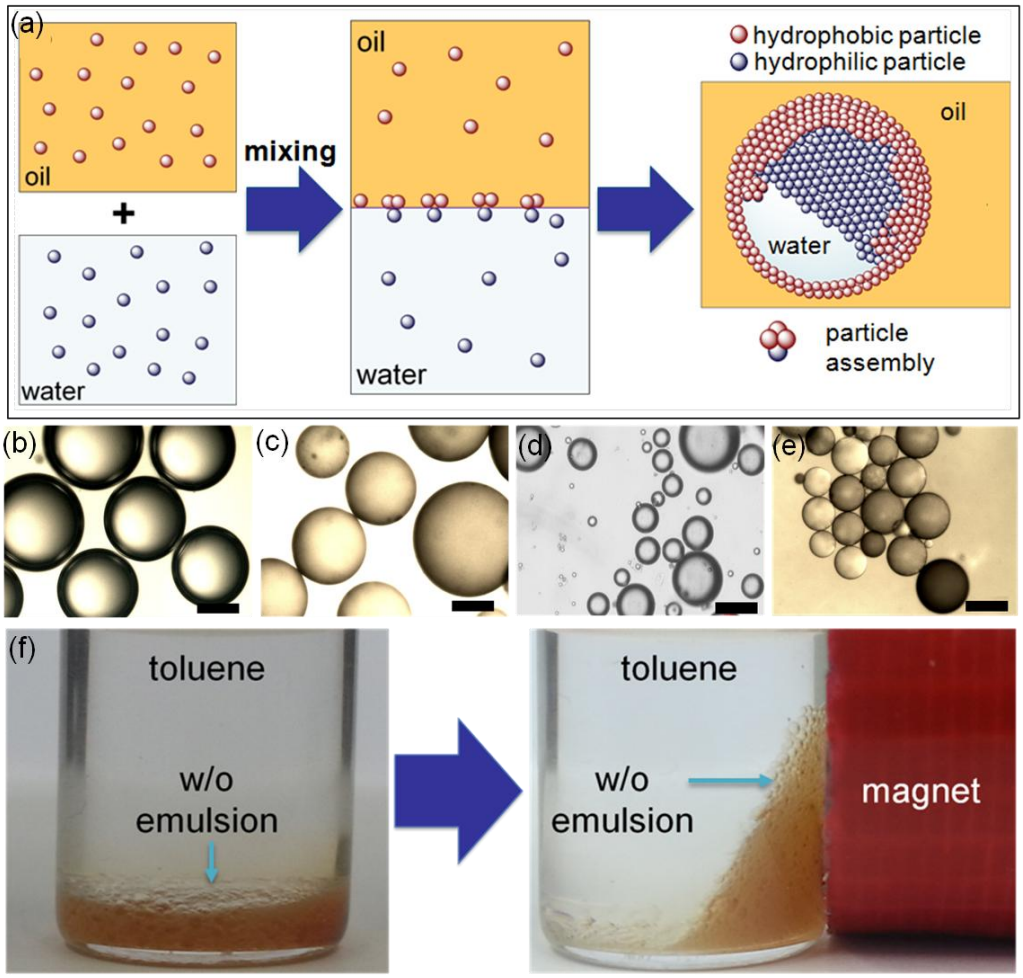


**Figure 2**. **(a)** Schematic showing how a water—in-oil emulsion can be stabilized by fully hydrophilic and fully hydrophobic particles assembling at the oil-water interface. 0.015 wt% suspensions were used in all experiments. Optical micrograph of **(b) a** water–in–toluene emulsion formed by mixing with hydrophilic CB suspension in water with hydrophobic fumed silica particles suspended in toluene, at a 3:7 volume ratio, **(c)** a toluene-in-water emulsion formed by these particles for aqueous suspension to toluene suspension volumetric ratio of 7:3. Optical micrographs of emulsions stabilized by spherical hydrophilic iron oxide particles in water and spherical hydrophobic silica particles in toluene showing **(d) a** water in-toluene emulsion formed with aqueous suspension to toluene suspension volume ratio of 3:7, **(e)** toluene-in-water emulsion formed when the spherical particle containing suspensions are mixed at a ratio of 7:3. Scale bars are 100μm. **(f)** Water-in-toluene emulsion stabilized by hydrophilic iron oxide and hydrophobic silica under the influence of magnetic field.

used 10nm diameter spherical iron oxide particles suspended in water at 0.015%w/w and 80nm diameter spherical silica particles suspended in toluene at 0.015%w/w, and formed W/O emulsions when mixed at a 30:70 ratio, as shown in Fig. 2(d). When the

balance of the aqueous to the oil phase is changed to 70:30 for this set of suspensions, an O/W emulsion is formed, shown in Fig. 2(e). In Fig. 2(f), we show that emulsion droplets made using iron oxide can be mobilized using magnets. Experiments are also performed where volume of oil and water is kept constant, but the ratio of wt% particles in these phases is kept at either 3:7 or 7:3. When the ratio of hydrophobic to hydrophilic particle is 7:3 we get water in oil emulsion and when this ratio is 3:7 oil in water emulsion is obtained. This is applicable both for fractal, spherical particles and is illustrated in Fig. 3.

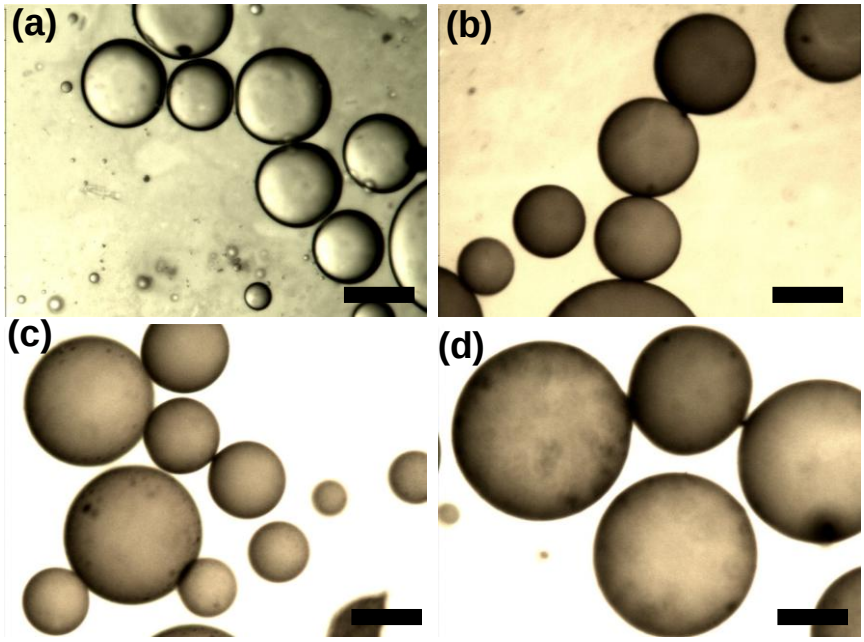


**Figure 3**. Optical micrograph of **(a)** a water–in–toluene emulsion formed by mixing equal volumes of water, oil containing hydrophilic CB and hydrophobic fumed silica particles respectively at a 3:7 weight ratio, **(b)** a toluene-in-water emulsion formed by using hydrophilic CB to hydrophobic fumed silica at a weight ratio of 7:3. Optical micrographs of emulsions stabilized by spherical hydrophilic iron oxide particles in water and spherical hydrophobic silica particles in toluene showing **(c)** a water-in-toluene emulsion formed with hydrophilic iron oxide to hydrophobic silica weight ratio of 3:7 and (d) a toluene-in-water emulsion formed by using hydrophilic iron oxide to hydrophobic silica at a weight ratio of 7:3. Scale bars are 100μm.

Fig. 4(a) shows a cryo-SEM image of a toluene drop stabilized by hydrophobic fumed silica and hydrophilic carbon black particles. The fracture plane is magnified in

Fig. 4(b). The layer of fumed silica particles is visible in the bottom left region, while the CB particles covering the fumed silica layer is visible on the upper right. The CB and fumed silica particles form supraparticle complexes at the toluene-water interface. Figures 4(c) and 4(d) are cryo-SEM images of oil drops stabilized by 80nm spherical hydrophobic silica and 10nm spherical hydrophilic iron oxide particle assemblies. Assembled silica and iron oxide particles are visible at the oil-water interface.

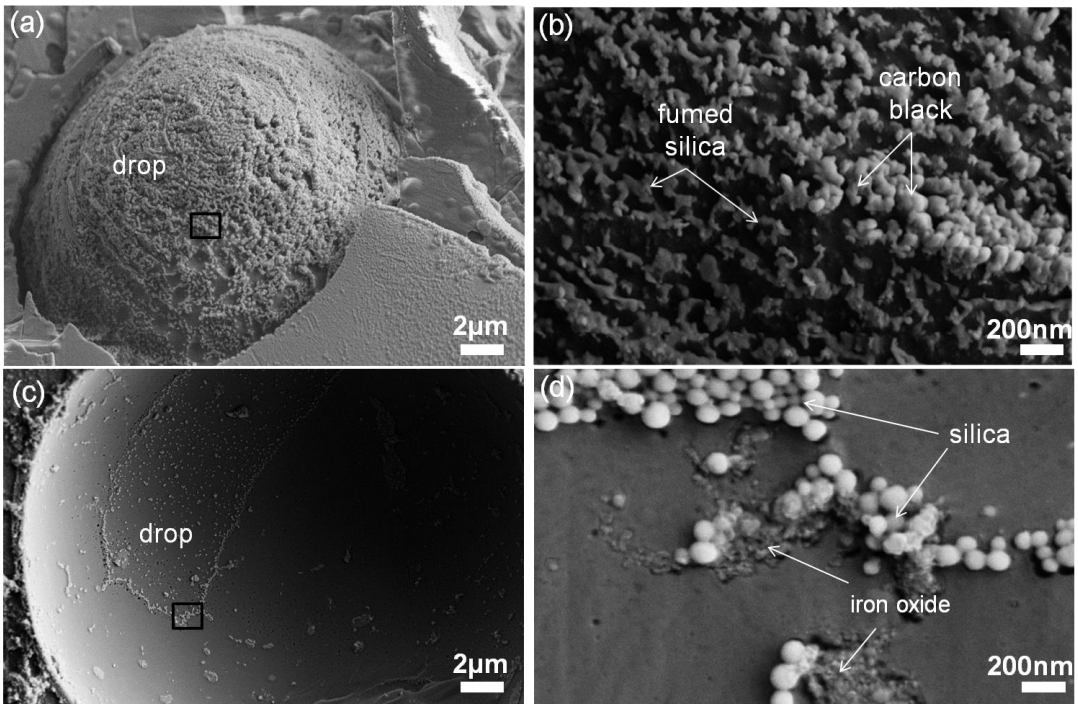


**Figure 4**. Cryo SEM images showing **(a)** an oil drop stabilized by particles, **(b)** higher magnification image of the fractured surface of the toluene drop. The CB particles form a top layer, shown on the upper right and fumed silica particles form an inner layer, shown on the lower left **(c)** a freeze fractured drop with spherical silica – iron oxide particles at the interface and **(d)** higher magnification perspective of the toluene-water interface showing silica –iron oxide assemblies at the interface.

An 80 vol% PEG 200 solution in water and a 90 vol% p-xylene solution in toluene have Hamaker constants of $6.63 \times 10^{-20}$J and $6.85 \times 10^{-20}$J respectively,[18] each higher than the Hamaker constant for silica, but lower than that of carbon or iron oxide. When stable suspensions of the hydrophilic and hydrophobic particles in these media

are mixed, they do not form an emulsion. Repulsive interactions between the hydrophilic and hydrophobic particle prevents formation of the partially wettable supraparticle aggregates that can stabilize emulsions.

We compare the energetics of emulsion formation using single particle suspensions to that using our technique. We lowered the pH of carbon black particles to 3.0 to make them partially wettable, so they can stabilize an emulsion.[19] This change in pH protonates the surface carboxylic groups and makes the CB partially hydrophobic. This initiates particle agglomeration. In addition, a particle network forms in the aqueous phase and increases the viscosity of the suspension. 30 vol% toluene is then added and vortexed to form an emulsion. The measured power consumption for emulsion formation over 1 minute is 22.1 watts. For our CB/silica case where we form emulsions using the same ratio of toluene to water, the power consumption over 1 minute is 7.8 watts. We suggest that the additional energy required to form emulsions in the partially wettable, single particle case is expended in breaking up aggregates or the CB network.

### 3.6 Conclusions

We demonstrate that when suspensions of completely hydrophilic particles in water and hydrophobic particles in toluene are mixed, attractive van der Waals interactions between these types of particles cause them to assemble into aggregates that are partially wettable in both phases. These entities are very effective at stabilizing emulsions. Both, water-in-toluene and toluene-in-water emulsions can be formed using the same sets of particles. The choice of particles and liquids is guided by

calculations of van der Waals interaction between a hydrophilic and hydrophobic particle through water and oil. Our experiments suggest that the energy expended to form an emulsion using this dual particle method is lower than that required when a single particle type is used to stabilize an emulsion. This strategy for forming particle-stabilized emulsions provides a powerful platform for developing new materials, with functionalities that are dictated by the types of particles in the emulsion.

### 3.7 Acknowledgements

We thank the financial support by the Gulf of Mexico Research Initiative and the University of Rhode Island Graduate Fellowship Program. We gratefully acknowledge discussions with Dr. Ashutosh Sharma.

### References

1. Ramsden, W. The separation of solid materials on surface of solutions and suspensions. Observations concerning surface diaphragms, emulsions and mechanical coagulation. [machine translation]. *Proc. Royal Soc. London* 1903, 72, 156-64.

2. Pickering, S. U. Emulsions. *J. Chem. Soc., Trans.* 1907, 91, 2001-21.

3. Finkle, P.; Draper, H. D.; Hildebrand, J. H. The theory of emulsification. *J. Am. Chem. Soc.* 1923, 45, 2780-8.

4. Schulman, J. H.; Leja, J. Control of contact angles at the oil-water-solid interfaces. Emulsions stabilized by solid particles (barium sulfate). *Trans. Faraday Soc.* 1954, 50, 598-605.

5. Binks, B. P., Horozov, T. S. *Colloidal Particles at Liquid Interfaces*. Cambridge University Press: 2008.

6. McGorty, R.; Fung, J.; Kaz, D.; Manoharan, V. N. Colloidal self-assembly at an interface. *Materials Today (Oxford, United Kingdom)* 2010, 13, 34-42.

7. Lee, D.; Weitz, D. A. Double emulsion-templated nanoparticle colloidosomes with selective permeability. *Adv. Mater. (Weinheim, Ger.)* 2008, 20, 3498-3503.

8. Reincke, F.; Kegel, W. K.; Zhang, H.; Nolte, M.; Wang, D.; Vanmaekelbergh, D.; Moehwald, H. Understanding the self-assembly of charged nanoparticles at the water/oil interface. *Physical Chemistry Chemical Physics* 2006, 8, 3828-3835.

9. Reincke, F.; Hickey, S. G.; Kegel, W. K.; Vanmaekelbergh, D. Spontaneous assembly of a monolayer of charged gold nanocrystals at the water/oil interface. *Angewandte Chemie, International Edition* 2004, 43, 458-462.

10. Larson-Smith, K.; Jackson, A.; Pozzo, D. C. SANS and SAXS Analysis of Charged Nanoparticle Adsorption at Oil-Water Interfaces. *Langmuir* 28, 2493-2501.

11. Amalvy, J. I.; Armes, S. P.; Binks, B. P.; Rodrigues, J. A.; Unali, G. F. Use of sterically-stabilised polystyrene latex particles as a pH-responsive particulate emulsifier to prepare surfactant-free oil-in-water emulsions. *Chemical Communications (Cambridge, United Kingdom)* 2003, 1826-1827.

12. Wang, H.; Singh, V.; Behrens, S. H. Image Charge Effects on the Formation of Pickering Emulsions. *Journal of Physical Chemistry Letters* 2012, 3, 2986-2990.

13. Israelachivili, J. N. *Intermolecular and surface forces*. Second ed.; Academic Press: 2005.

14. Tadmor, R. The London-van der Waals interaction energy between objects of various geometries. *Journal of Physics: Condensed Matter* 2001, 13, L195-L202.

15. Vold, M. J. The effect of adsorption on the van der Waals interaction of spherical colloidal particles. *Journal of Colloid Science* 1961, 16, 1-12.

16. Vincent, B. The van der Waals attraction between colloid particles having adsorbed layers. II. Calculation of interaction curves. *Journal of Colloid and Interface Science* 1973, 42, 270-85.

17. Ebaadi, S. H. Van der Waals interaction between surfactant-coated and bare colloidal particles. *Colloids and Surfaces* 1981, 2, 155-68.

18. Saunders, S. R.; Anand, M.; You, S.-S.; Roberts, C. B. Total interaction energy model to predict nanoparticle dispersability in CO2-expanded solvents. *Computer-Aided Chemical Engineering* 28, 1651-1656.

19. Saha, A.; Nikova, A.; Venkataraman, P.; John, V. T.; Bose, A. Oil Emulsification Using Surface-Tunable Carbon Black Particles. *ACS Applied Materials & Interfaces* 2013, 5, 3094-3100.

20. Johnson, J. E.; Belmont, J. A. Modified colored pigments and ink jet inks, and coatings containing modified pigments. 1997-871453, 5922118, 19970609, 1999.

21. Hosokawa, M.; Nogi, K.; Naito, M.; Yokoyama, T.; Editors. *Nanoparticle Technology Handbook*. Second ed.; Elsevier: 2012; p 703 pp.

22. Hiemenz, P., C. *Principles of Colloid and Surface Chemistry*. Second ed.; New York and Basel, 1986.

# CHAPTER 4

## New Insights into the transformation of Calcium Sulfate Hemihydrate to Gypsum using time-resolved Cryogenic Transmission Electron Microscopy

(published in Langmuir, 2012, 28 (30), pp 11182–11187)

Amitesh Saha,[†] Jinkee Lee,[ϒ] Sabrina M. Pancera,[§] Michael F. Bräeu,[‡] Andreas Kempter,[§] Anubhav Tripathi,[ǂ] Arijit Bose[*†]

[†]Department of Chemical Engineering, University of Rhode Island, Kingston, RI 02881, USA

[ϒ]School of Mechanical Engineering, Sungkyunkwan University, Suwon, 440-746, Korea

[ǂ]School of Engineering, Brown University, Providence, RI 02906, USA,

[§]BASF SE, 67056 Ludwigshafen, Germany,

[‡]BASF Construction Chemicals GmbH, 83308 Trostberg, Germany,

*Corresponding author: tel: 401-874-2804, email: bosea@egr.uri.edu

## 4.1 Abstract

We use time-resolved cryogenic transmission electron microscopy (TR-cryo-TEM) on a supersaturated solution of calcium sulfate hemihydrate to examine the early stages of particle formation during the hydration of the hemihydrate. As hydration proceeds, we observe nanoscale amorphous clusters that evolve to amorphous particles and then reorganize to crystalline gypsum within tens of seconds. Our results indicate that a multi-step particle formation model, where an amorphous phase forms first, followed by the transformation into a crystalline product, is applicable even at time scales of the order of tens of seconds for this system. The addition of a small amount of citric acid significantly delays the reorganization to gypsum crystals. We hypothesize that available calcium ions form complexes with the acid by binding to the carboxylic groups. Their incorporation into a growing particle produces disorder, and extends the time over which the amorphous phase exists. We see evidence of patches of 'trapped' amorphous phase within the growing gypsum crystal at time scales of the order of 24 hours. This is confirmed by complementary X-ray diffraction experiments. Direct imaging of nanoscale samples by TR-cryo-TEM is a powerful technique for a fundamental understanding of crystallization, and many other evolving systems.

## 4.2 Introduction

While crystal growth from supersaturated solutions has been studied extensively, we use time-resolved cryogenic transmission microscopy to provide new insights into the hydration of calcium sulfate hemihydrate ($CaSO_4 \cdot 0.5H_2O$) to form gypsum

($CaSO_4 \cdot 2H_2O$). Cryo-TEM has been used previously to examine calcium carbonate formation, both in free solution[1] and by templating,[2, 3] and for studying early stages of iron oxide formation.[4] The transformation of calcium sulfate hemihydrate to gypsum has been a topic of considerable interest because of its application in the construction and medical industries, but little is known about particle shapes and phases existing at the very early stages of this process,[5] which in turn, affects the existence of subsequent phases and morphologies. Insight into this process also has implications for understanding biological mineralization.[6] Gypsum, formed by mixing calcium chloride and sodium sulfate solutions has been studied recently,[7] and an amorphous precursor to the final crystalline phase has been observed. We trigger crystallization on a single supersaturated solution rather than mixing two solutions, removing the potential for any mixing induced artifacts. In combination with careful sample preparation for cryo-TEM, the observed transformations become material-based and not processing related. Quenching the sample also allows us to conveniently probe the transformation at well-defined short time scales and small length scales. Since this transformation occurs by a hydration reaction, any consequences of electron beam induced dehydration can be identified easily and data from those experiments are eliminated. Time-resolved cryo-TEM therefore offers some important advantages over other probing techniques, including imaging of nanoscale objects in real space in their native environment.

We follow the reaction:

$$2\ CaSO_4 \cdot 0.5H_2O + 3\ H_2O \rightarrow 2\ CaSO_4 \cdot 2H_2O + \text{Heat}, \qquad (1)$$

culminating in the formation and growth of calcium sulfate dihydrate, or gypsum, crystals. When this reaction occurs in pastes, it produces plaster, a porous material with high internal surface area containing interlocking crystals in the form of needles and plates.[8] The morphology and size of gypsum in the hardened paste affects its compressive strength. In the plaster and building industries,[9] additives (accelerators or retardants) are used to control the hemihydrate hydration rate in order to influence the morphology and size scales of the end material. Splints as well as plasters used for medical applications need rapid buildup with high final compressive strength, and hence require accelerators.[10] On the other hand, scaling inside seawater desalination plants, pipes, boilers, heat exchangers, cooling water systems and secondary oil recovery systems is caused by the precipitation and growth of inorganic salts,[5] and should be suppressed. Addition of organic, inorganic or polymeric additives such as polycarboxylates and polyphosphonates[11,12, 13] are often used to reduce scaling.

Classical nucleation theory predicts that the earliest particles that form have the crystal structure of the end product. On the other hand, a two-step model[14] first allows for the formation of disordered clusters which are less constrained than crystalline phases. This is followed by reorganization to ordered crystalline domains. Another study[15] using electron microscopy has shown that the transformation of amorphous calcium phosphate spheres to crystalline spherulites occurs via a multi step surface nucleation process. Studies on model colloidal systems[16-18] have also indicated deviation from classical nucleation theory. Thus it is important to distinguish between classical nucleation models and the applicable crystallization mechanisms for specific systems.[19]

From a practical perspective, an understanding of the precipitation/crystallization processes is essential so that additives can be rationally designed. This insight can be obtained by examining the temporal evolution of the crystal habit. Light microscopy, scanning electron microscopy and atomic force microscopy have been deployed for this purpose.[20, 21] Although, their spatial resolution is often adequate, these methods typically require samples that are several microns in size. Additionally, these methods do not easily lend themselves sample 'quenching' making it difficult to capture particles in their native states at short and specific time points. Consequently, the sampled particles are usually well beyond the initial stages of transformation. Therefore, crucial information about phase and morphology that is embedded in the very early stages of crystal growth is lost. This issue becomes even more important when the effect of additives[22-27] must be understood, as they strongly influence the very early stages of particle formation and growth. A more complete understanding of the interaction between additive molecules and initial particle formation can be greatly aided by direct probing techniques at very early time points. These interactions provide vital information about the evolution of the crystallization process in the presence of additives. This understanding will guide the choice of additives for either accelerating or retarding the crystallization process depending on the applications. Intrinsically coupled with short time scales is the small (sub-micron) length scales for these growing particles, which requires alternate techniques for direct imaging and analysis. Conventional methods[28-32] therefore give only a late-stage picture of the influence of additives on the crystallization process. Time-resolved X-ray scattering using a strong beam source [33,34] is a viable technique for examining particle evolution

at short time scales. However, this method produces data in reciprocal space, and does not produce direct real-time morphologies of particles.

We use time resolved cryogenic transmission electron microscopy (TR-cryo-TEM) as our primary probing technique to get detailed insight on the early stages of the transformation of calcium sulfate hemihydrate to gypsum. Vitrification of samples is an artifact-free way to quench the system, allowing both morphology and phase (via electron diffraction) information to be captured at a specific time point. Particle sizes are in the range of tens of nanometers, ideally suited for examination by transmission electron microscopy. In our experiments, a supersaturated solution of calcium sulfate hemihydrate is filtered to trigger crystallization, subsequently quenched and examined at various time points after the filtering. We have also examined the influence of citric acid on gypsum crystallization using this technique, as carboxylic acids are some of the most commonly used additives for modulating gypsum formation.

## 4.3 Materials

Calcium sulfate hemihydrate (98%) (12090-1KG-R) ($CaSO_4 \cdot 0.5H_2O$) was obtained from Sigma Aldrich. Citric acid (99+ %) was purchased from Alfa Aesar.

## 4.4 Methods

### 4.4.1 Preparation of sample solutions

Powdered calcium sulfate hemihydrate is rapidly stirred into distilled deionized water (Milli Q – resistance 18MΩ). It is then filtered to obtain a supersaturated solution and to remove any undissolved hemihydrate particles. Filtration also triggers the crystallization process. The filtrate is vitrified at different time points ranging from 10 seconds to 60 seconds after filtration. To get an insight into the effect of additives

on the early stages of gypsum crystallization, a 2.6mM citric acid solution is added to the solution of calcium sulfate hemihydrate. This is followed by filtration and vitrification at different time points.

In order to determine the concentration of the hemihydrate solution after filtration, a known volume of the filtrate is withdrawn, and heated to 90°C for 8 hrs. This heat treatment partially dehydrates gypsum, and transforms it back to the hemihydrate. The residual dry powder is weighed, and used to calculate the concentration of hemihydrate in solution. The measured concentration of the calcium sulfate hemihydrate in the filtrates for the cases without additive varies between 52mM and 58mM for all our samples. Taking a mean concentration of 55 mM gives a supersaturation ratio of 2.85. For experiments to study the effect of citric acid on gypsum crystallization, we get hemihydrate concentrations that vary between 58mM and 66mM with a mean of 62mM.

**4.4.2** Sample Preparation for cryo-TEM

A few microliters of the solution are deposited on to a holey carbon cryo-TEM grid. The grid is carefully blotted so that liquid bridges of the order of 100 nm in thickness are formed across the holes. The grid is then plunged into a liquid ethane reservoir cooled by liquid nitrogen. Rapid heat transfer away from the solution on the grid leads to vitrification. The wait time after filtration is managed carefully so that the sample gets vitrified at a desired time point. This entire operation is done in a controlled environment vitrification system (CEVS) maintained at 25°C and at 100% humidity to prevent water evaporation from the sample prior to vitrification.

**4.4.3** Characterization

The grid-containing sample is transferred to a cooled tip of a Gatan 626 DH cryo transfer stage. The stage is then inserted into a JEOL JEM 2100 Transmission Electron Microscope. The sample is maintained at -175 ° C and low electron dosage is used for probing the samples to prevent the amorphous to crystalline phase transformation in ice as well as any potential dehydration. An Oxford Instruments Inca EDX system is used for elemental analysis. Selected area electron diffraction (SAED) is performed on regions of interest to get phase information. X-ray diffraction (XRD) patterns from our samples are recorded using a Rigaku Ultima IV diffractometer. The samples are kept in a holder and sealed using a thin plastic film to prevent drying during measurements.

**4.5 Results and Discussion**

To investigate gypsum crystallization, a 55mM supersaturated solution of calcium sulfate hemihydrate is vitrified at different time points. Samples vitrified approximately 10 seconds after filtration show the presence of 2nm - 4nm particles, as indicated in Fig. 1. Low-dose selected area electron diffraction (SAED) for these

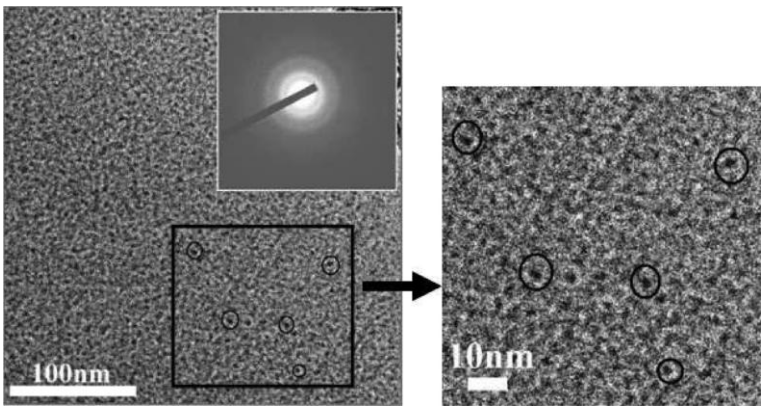


**Figure 1.** Cryo-TEM image (left) of sample solution vitrified 10 seconds after filtration showing particles (few encircled). A higher magnification image of the marked area is shown on the right. The inset in the left cryo TEM micrograph is a selected area electron diffraction (SAED) image showing diffuse diffraction pattern, an indication of amorphous phase.

particles results in a diffuse diffraction pattern (inset), indicating an amorphous phase. These are nanoscale amorphous clusters. At intermediate times of the order of 15 seconds, we observe larger particles (Figs. 2(a), 2(b), 2(c)). Figs. 2(d), (e), (f) are SAED patterns from these particles.

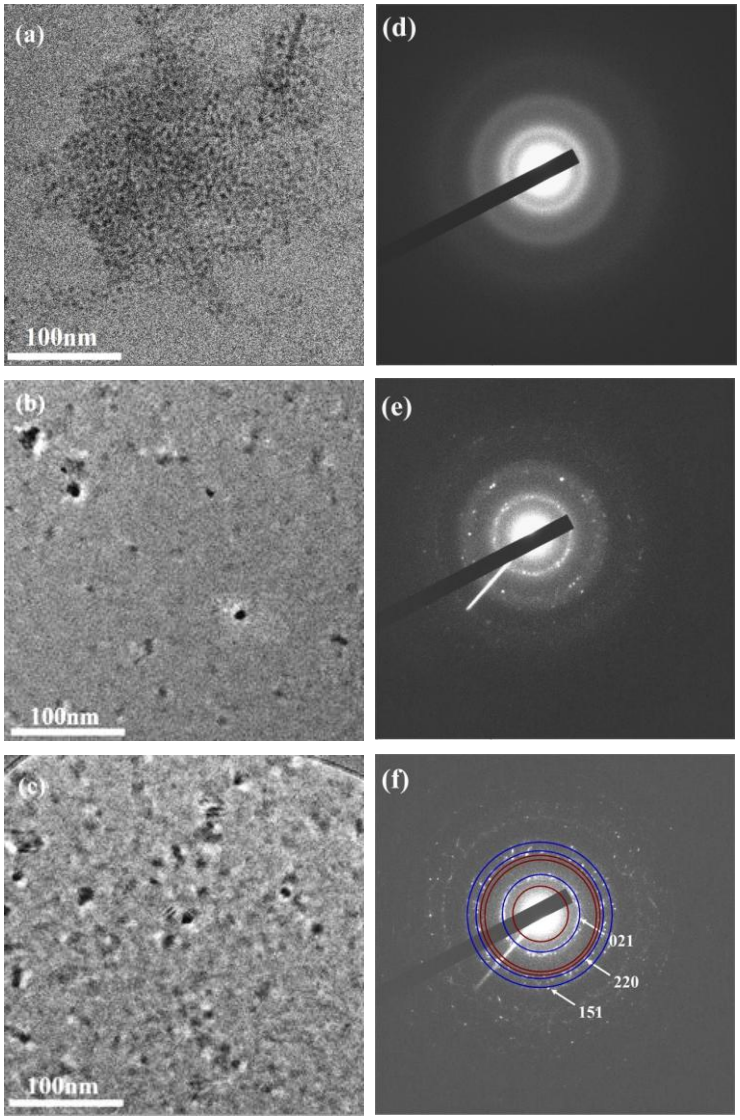


**Figure 2.** Cryo-TEM micrographs of a sample solution aged for 15 seconds after filtration. Different regions of the image show **(a)** amorphous nanoparticles, **(b)** and **(c)** increasingly agglomerated nanoparticles respectively. Corresponding SAED patterns are shown on adjacent figures **(d)** diffuse diffraction pattern, **(e)** more distinct diffraction rings, indicating an increase in crystallinity and **(f)** diffraction rings (marked in blue) that index to gypsum; the red circles indicate locations where the rings corresponding to the hemihydrate would appear. At 15 seconds, there is a coexistence of amorphous and crystalline nanoparticles throughout the TEM grid.

We observe characteristic rings indicating an increase in crystallinity. These rings can be indexed to gypsum. After about 15 seconds, reorganization of the amorphous particles to a crystalline phase has begun. We note that EDX done on the particles always reveals the presence of calcium and sulfur. Thus the particles seen in these figures are not an artifact of diffraction contrast caused by an amorphous to cubic phase transformation in the vitrified background film.

Fig. 3(a) shows particles in a sample vitrified 20 seconds after filtration. SAED on these particles confirm the presence only of gypsum as shown in Fig. 3(b). These particles eventually evolve to micron- and then millimeter-sized needle-like structures characteristic of gypsum.[30, 35] Cryo-TEM images at 30 seconds, 60 seconds have consistently shown the presence of acicular particles typical of gypsum.

During the early stages, amorphous nanoparticles evolve from nanoscale amorphous clusters.[2, 36, 37] These nanoparticles grow. The amorphous state is favored kinetically because it is less constrained than the crystalline counterpart, but it is not one of minimum free energy. Thus, the disordered state slowly rearranges to more stable crystalline form, gypsum. A transient amorphous phase is not predicted by classical nucleation theory. In Fig. 3(c), we show an alternate multi-step mechanism for the transformation of the hemihydrate to gypsum, more closely corresponding to our observations. We have subsequently followed the evolution of morphology of these particles from 15 min to an hour and observe typical interlocking needle-like gypsum.

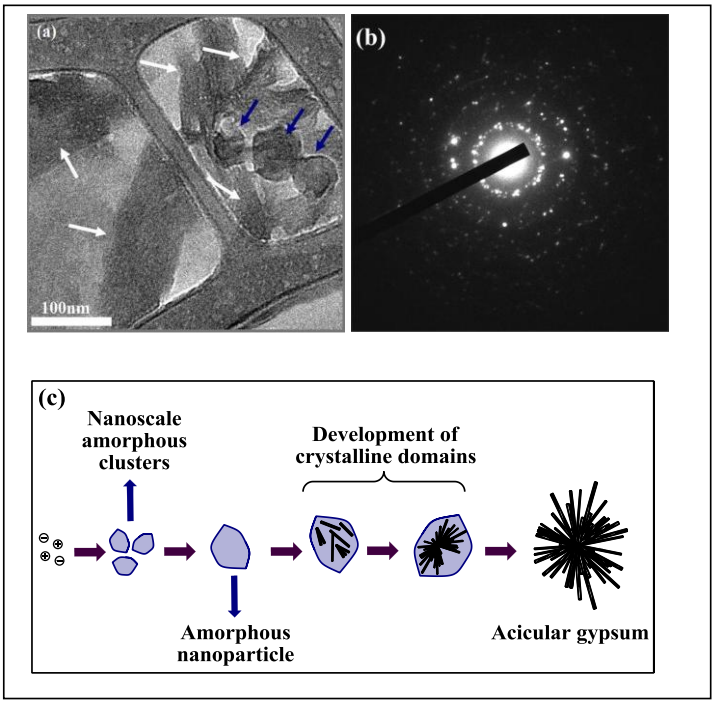


**Figure 3. (a)** Cryo-TEM image of a sample solution vitrified 20 seconds after filtration showing gypsum (marked by white arrows), blue arrows refer to frost particles **(b)** SAED confirming presence of crystalline gypsum (calcium sulfate dihydrate) **(c)** our proposed model for the early stages of gypsum formation.

We use citric acid as a model additive for gypsum crystallization and prepare a supersaturated solution of calcium sulfate hemihydrate (62mM) containing 2.6mM of the acid. A sample solution vitrified 10 seconds after filtration is shown in Fig. 4(a). A diffuse diffraction pattern (Fig. 4(b)) confirms the presence of an amorphous phase throughout the sample.

Even at 60 seconds after filtration we observe only amorphous particles, as shown by the diffraction patterns in Figs. 4(c) and 4(d), confirming that citric acid has a strong retarding effect on gypsum formation from the hemihydrate. EDX from these particles give peaks of Ca, O, C and S. Ionized carboxylic groups and available calcium ions interact to form complexes. Structural matching between two oxygen atoms in neighboring carboxylate groups in citric acid and two calcium atoms on

gypsum has been considered to play a pivotal role in complex formation[29]. Adsorption of these complexes onto a growing particle, introduces disorder, and delays the crystallization process. Adsorption of carboxylic acids on the surface of calcium sulfate dihydrate has been confirmed previously by DSC and FTIR[31]. ICP measurements[38] of calcium and sulfate ion concentrations with and without citric acid have also supported the idea of complex formation.

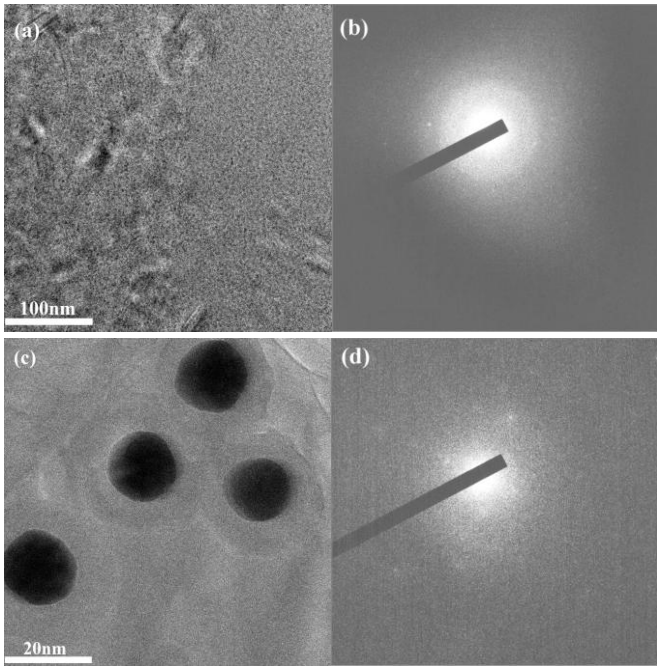


**Figure 4. (a)** Cryo-TEM micrograph of a sample containing 2.6mM citric acid, 62mM calcium sulfate hemihydrate at 10 seconds after filtration **(b)** Electron diffraction showing diffuse rings-an indication of amorphous phase **(c)** Cryo-TEM image of a sample vitrified 60 seconds after filtration – note the absence of acicular particles **(d)** Electron diffraction showing diffuse pattern indicating an amorphous structure.

Optical micrographs taken at 60 minutes show no acicular structures, confirming the retardation of the crystallization process. Images taken at 24 hrs however, (Fig. 5) show acicular structures projecting from a dense internal phase similar to structures reported previously.[39]

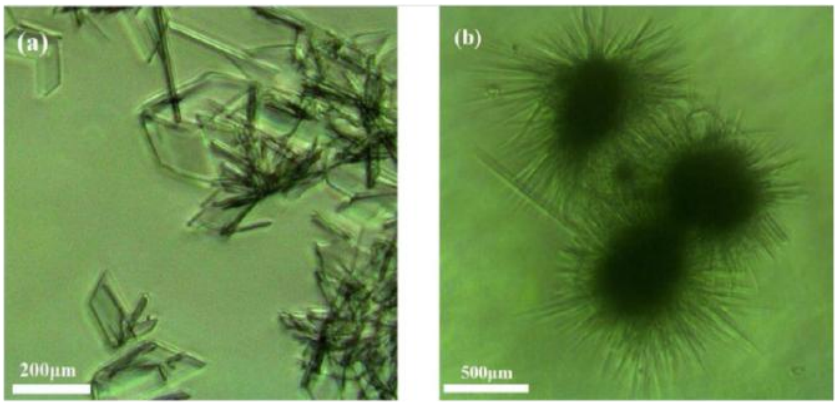


**Figure 5.** Optical microscope images of samples containing **(a)** no additives, 24 hrs after filtration showing large acicular crystals and **(b)** 2.6mM citric acid, analyzed 24 hrs after filtration. The interior of the particles in (b) show a different morphology from case (a).

Cryo-TEM images of these needles are shown in Fig. 6. Interestingly, electron diffraction on area 1 gives a diffuse pattern indicating a disordered amorphous phase (top right inset in Fig. 6). EDX from that area give peaks of Ca, O and C only and no S. Electron diffraction patterns from a region near the edge of the acicular structures (marked in Fig. 6) match gypsum. EDX gives peaks of Ca, S, O and C. We find such a combination of amorphous and crystalline structures persisting throughout the sample at this time point. Our results indicate that these acicular structures consist of trapped amorphous phases that are predominantly composed of Ca, O and C along with crystalline gypsum. Complexes formed at earlier time points induce disorder into the system and retard the crystallization process. However, crystalline gypsum eventually becomes the predominant phase, although we still see patches of amorphous phase at 24 hrs.

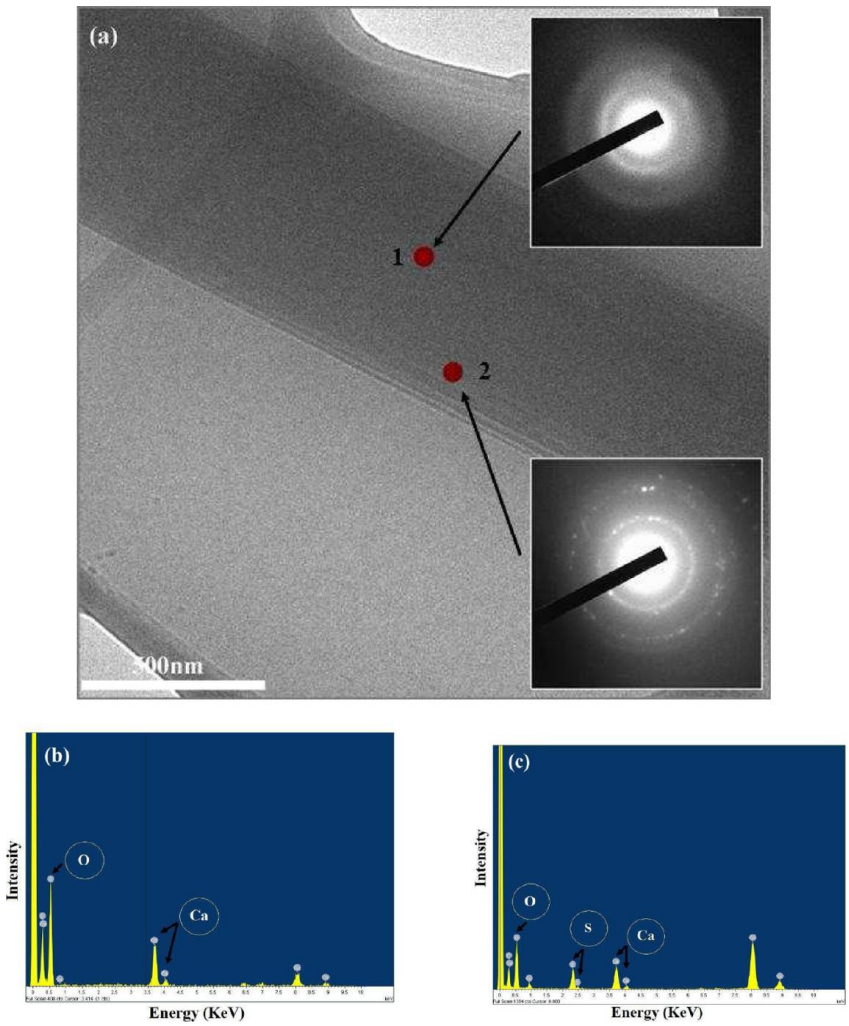


**Figure 6. (a)** Cryo-TEM image of sample showing a portion of an acicular structure formed in the citric acid addition experiments. Samples are observed at 24 hrs. The insets show electron diffraction patterns from the regions marked by the red dots, indicating (top right) a disordered amorphous phase in region 1 (no spots corresponding to crystals) and (bottom right) gypsum in region 2 (diffraction spots indicate crystal formation, the spots index to gypsum). EDX showing **(b)** Ca, O, C in region 1 and **(c)** Ca, O, C, S in region 2.

XRD measurements on particles in solution at different time points corroborate our findings. Figure 7 shows X-ray diffraction patterns for particles at 24 hours after filtration. For the citric acid containing samples, we focus on the intense [0 2 0] gypsum peak[40] to allow statistically meaningful data collection in a few minutes. In the presence of citric acid at 24 hours (Figure 7) we see the formation of a very low intensity [0 2 0] peak indicating the growth of the gypsum crystalline domains at

around this time point. In contrast, at earlier time points, we see a featureless diffraction pattern in these samples.

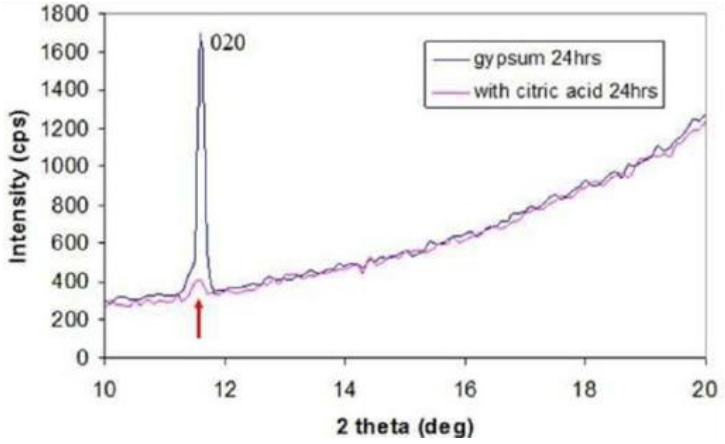


**Figure 7.** XRD diffraction patterns of a hemihydrate solution at 24 hrs, showing an intense [0 2 0] peak of gypsum (blue) when there are no additives, and a very low intensity peak (red arrow) matching with [0 2 0] gypsum peak in presence of citric acid.

### 4.6 Conclusions

We demonstrate how time-resolved cryogenic transmission electron microscopy can be a powerful technique for the understanding of early time evolution of the calcium sulfate hemihydrate to gypsum hydration process, and the effect of the additive, citric acid, on resulting particle phases. Cryo-TEM allows structures to be trapped in native states, and physically quenches the system, important for understanding morphology and phase behavior at important length (size) scales. For the formation of gypsum from the hemihydrate, we report the existence of nanoscale amorphous clusters, which are the building blocks of amorphous nanoparticles. Crystalline domains are formed within these amorphous particles. The energetically favorable crystalline phase evolves eventually. A multi-step model describes this system more accurately than classical nucleation theory. Even at low concentrations, citric acid inhibits gypsum nucleation and growth by the development of a disordered amorphous phase formed

by the association of the carboxyl groups with calcium ions. The effect of citric acid on delaying crystallization in this system persists up to 24 hours.

### 4.7 Acknowledgements

The authors gratefully acknowledge support from the National Science Foundation (CBET 0730392, 0854115) and from BASF.

### References

1. Rieger, J.; Frechen, T.; Cox, G.; Heckmann, W.; Schmidt, C.; Thieme, J., Precursor structures in the crystallization/precipitation processes of CaCO3 and control of particle formation by polyelectrolytes. *Faraday Discussions* **2007,** 136, 265-277.

2. Pouget, E. M.; Bomans, P. H. H.; Goos, J. A. C. M.; Frederik, P. M.; de With, G.; Sommerdijk, N. A. J. M., The Initial Stages of Template-Controlled CaCO3 Formation Revealed by Cryo-TEM. *Science (Washington, DC, United States)* **2009,** 323, (5920), 1455-1458.

3. Pichon, B. P.; Bomans, P. H. H.; Frederik, P. M.; Sommerdijk, N. A. J. M., A Quasi-Time-Resolved CryoTEM Study of the Nucleation of CaCO3 under Langmuir Monolayers. *Journal of the American Chemical Society* **2008,** 130, (12), 4034-4040.

4. Yuwono, V. M.; Burrows, N. D.; Soltis, J. A.; Penn, R. L., Oriented Aggregation: Formation and Transformation of Mesocrystal Intermediates Revealed. *Journal of the American Chemical Society* **2010,** 132, (7), 2163-2165.

5. Singh, N. B.; Middendorf, B., Calcium sulphate hemihydrate hydration leading to gypsum crystallization. *Progress in Crystal Growth and Characterization of Materials* **2007,** 53, (1), 57-77.

6. Oner, M.; Dogan, O.; Oner, G., The influence of polyelectrolytes architecture on calcium sulfate dihydrate growth retardation. *Journal of Crystal Growth* **1998,** 186, (3), 427-437.

7. Wang, Y.-W.; Kim, Y.-Y.; Christenson, H. K.; Meldrum, F. C., A new precipitation pathway for calcium sulfate dihydrate (gypsum) via amorphous and hemihydrate intermediates. *Chemical Communications (Cambridge, United Kingdom)* **2012,** 48, (4), 504-506.

8. Triollier, M.; Guilhot, B., The hydration of calcium sulfate hemihydrate. *Cement and Concrete Research* **1976,** 6, (4), 507-14.

9. Middendorf, B.; Vellmer, C.; Schmidt, M., Take a closer look: Calcium sulphate based building materials in interaction with chemical additives. *Special Publication - Royal Society of Chemistry* **2004,** 292, (Nanotechnology in Construction), 263-272.

10. Lewry, A. J.; Williamson, J., The setting of gypsum plaster. Part III. The effect of additives and impurities. *Journal of Materials Science* **1994,** 29, (23), 6085-90.

11. Weijnen, M. P. C.; Van Rosmalen, G. M., Adsorption of phosphonates on gypsum crystals. *Journal of Crystal Growth* **1986,** 79, (1-3, [Pt. 1]), 157-68.

12. Van Rosmalen, G. M.; Daudey, P. J.; Marchee, W. G. J., An analysis of growth experiments of gypsum crystals in suspension. *Journal of Crystal Growth* **1981,** 52, (2), 801-11.

13. Akyol, E.; Oner, M.; Barouda, E.; Demadis, K. D., Systematic Structural Determinants of the Effects of Tetraphosphonates on Gypsum Crystallization. *Crystal Growth & Design* **2009,** 9, (12), 5145-5154.

14. Erdemir, D.; Lee, A. Y.; Myerson, A. S., Nucleation of Crystals from Solution: Classical and Two-Step Models. *Accounts of Chemical Research* **2009,** 42, (5), 621-629.

15. Pan, H.; Liu, X. Y.; Tang, R.; Xu, H. Y., Mystery of the transformation from amorphous calcium phosphate to hydroxyapatite. *Chemical Communications (Cambridge, United Kingdom)* **2010,** 46, (39), 7415-7417.

16. Zhang, T. H.; Liu, X. Y., Nucleation: what happens at the initial stage? *Angewandte Chemie, International Edition* **2009,** 48, (7), 1308-1312.

17. Zhang, T. H.; Liu, X. Y., How Does a Transient Amorphous Precursor Template Crystallization. *Journal of the American Chemical Society* **2007,** 129, (44), 13520-13526.

18. Zhang, T. H.; Liu, X. Y., Multistep Crystal Nucleation: A Kinetic Study Based on Colloidal Crystallization. *Journal of Physical Chemistry B* **2007,** 111, (50), 14001-14005.

19. Horn, D.; Rieger, J., Organic nanoparticles in the aqueous phase - theory, experiment and use. *Angewandte Chemie, International Edition* **2001,** 40, (23), 4330-4361.

20. Zhu, Y.; Demilie, P.; Davoine, P.; Cartage, T.; Delplancke-Ogletree, M.-P., Influence of calcium ions on the crystallization of sodium bicarbonate. *Journal of Crystal Growth* **2005,** 275, (1-2), e1333-e1339.

21. Finot, E.; Lesniewska, E.; Goudonnet, J. P.; Mutin, J. C., Correlation between surface forces and surface reactivity in the setting of plaster by atomic force microscopy. *Applied Surface Science* **2000,** 161, (3-4), 316-322.

22. Kruger, A.; Focke, W. W.; Kwela, Z.; Fowles, R., Effect of Ionic Impurities on the Crystallization of Gypsum in Wet-Process Phosphoric Acid. *Industrial & Engineering Chemistry Research* **2001,** 40, (5), 1364-1369.

23. Rashad, M. M.; Mahmoud, M. H. H.; Ibrahim, I. A.; Abdel-Aal, E. A., Crystallization of calcium sulfate dihydrate under simulated conditions of phosphoric acid production in the presence of aluminum and magnesium ions. *Journal of Crystal Growth* **2004,** 267, (1-2), 372-379.

24. Chatterji, A. K.; Kapse, G. W., Rheology of dilute aqueous suspensions of some reactive solids. *Nature (London, United Kingdom)* **1963,** 200, (4909), 868-70.

25. Brandt, F.; Bosbach, D., Bassanite (CaSO4Â·0.5H2O) dissolution and gypsum (CaSO4Â·2H2O) precipitation in the presence of cellulose ethers. *Journal of Crystal Growth* **2001,** 233, (4), 837-845.

26. Bosbach, D.; Hochella, M. F., Jr., Gypsum growth in the presence of growth inhibitors: a scanning force microscopy study. *Chemical Geology* **1996,** 132, (1-4), 227-236.

27. Song, R.-Q.; Colfen, H., Additive controlled crystallization. *CrystEngComm* **2011,** 13, (5), 1249-1276.

28. Boisvert, J. P.; Domenech, M.; Foissy, A.; Persello, J.; Mutin, J. C., Hydration of calcium sulfate hemihydrate (CaSO4.1/2H2O) into gypsum (CaSO4.2H2O). The

influence of the sodium poly(acrylate)/surface interaction and molecular weight. *Journal of Crystal Growth* **2000,** 220, (4), 579-591.

29. Badens, E.; Veesler, S.; Boistelle, R., Crystallization of gypsum from hemihydrate in presence of additives. *Journal of Crystal Growth* **1999,** 198/199, (Pt. 1), 704-709.

30. Lewry, A. J.; Williamson, J., The setting of gypsum plaster. Part I. The hydration of calcium sulfate hemihydrate. *Journal of Materials Science* **1994,** 29, (20), 5279-84.

31. Vellmer, C.; Middendorf, B.; Singh, N. B., Hydration of Î±-hemihydrate in the presence of carboxylic acids. *Journal of Thermal Analysis and Calorimetry* **2006,** 86, (3), 721-726.

32. Peng, J.; Qu, J.; Zhang, J.; Chen, M.; Wan, T., Adsorption characteristics of water-reducing agents on gypsum surface and its effect on the rheology of gypsum plaster. *Cement and Concrete Research* **2005,** 35, (3), 527-531.

33. Hanley, T.; Sutton, D.; Heeley, E.; Moad, G.; Knott, R., A small-angle X-ray scattering study of the effect of chain architecture on the shear-induced crystallization of branched and linear poly(ethylene terephthalate). *Journal of Applied Crystallography* **2007,** 40, (S1), s599-s604.

34. Chattopadhyay, S.; Erdemir, D.; Evans, J. M. B.; Ilavsky, J.; Amenitsch, H.; Segre, C. U.; Myerson, A. S., SAXS Study of the Nucleation of Glycine Crystals from a Supersaturated Solution. *Crystal Growth & Design* **2005,** 5, (2), 523-527.

35. Anderson, J. N., *Applied Dental Materials*. Blackwell: London, 1976.

36. Gebauer, D.; Voelkel, A.; Coelfen, H., Stable Prenucleation Calcium Carbonate Clusters. *Science (Washington, DC, United States)* **2008,** 322, (5909), 1819-1822.

37. Meldrum, F. C.; Colfen, H., Crystallization and formation mechanisms of nanostructures. *Nanoscale* **2010,** 2, (11), 2326-2327.

38. Ersen, A.; Smith, A.; Chotard, T., Effect of malic and citric acid on the crystallization of gypsum investigated by coupled acoustic emission and electrical conductivity techniques. *Journal of Materials Science* **2006,** 41, (21), 7210-7217.

39. Titiz-Sargut, S.; Sayan, P.; Avci, B., Influence of citric acid on calcium sulfate dihydrate crystallization in aqueous media. *Crystal Research and Technology* **2007,** 42, (2), 119-126.

40. Follner, S.; Wolter, A.; Helming, K.; Silber, C.; Bartels, H.; Follner, H., On the real structure of gypsum crystals. *Crystal Research and Technology* **2002,** 37, (2-3), 207-218.

# CHAPTER 5

## Understanding Impact of Perfume Raw Materials on the Evolution of Microstructures in Vesicular Dispersions relevant to Fabric Softeners

(in preparation for Langmuir)

Amitesh Saha,[†] Marc Mamak,[§] Anubhav Tripathi,[‡] Arijit Bose[†*]

† Department of Chemical Engineering, University of Rhode Island, Kingston, RI 02881, USA

‡ School of Engineering, Brown University, Providence, RI 02906, USA

§ Research and Development, Procter & Gamble, Cincinnati, OH 45202, USA

*Corresponding author: tel: 401-874-2804, email: bosea@egr.uri.edu

## 5.1 Abstract

We use time resolved cryogenic transmission electron microscopy to investigate the effect of perfume raw materials (PRMs) on the evolution of microstructures in commercial fabric softener Ultra Downy Free (UDF) spanning from 10 seconds to hours. For our study, linalyl acetate and eugenol are chosen. PRMs are delivered to UDF by probe sonication. Transitions in vesicular dispersions induced by the PRMs are carefully studied. When linalyl acetate is used, multilamellar vesicles in UDF are retained even at 24hrs. However, eugenol triggers a transition from multi lamellar vesicles to predominantly uni lamellar vesicles through bilayer breakage. Nuclear magnetic resonance experiments reveal that eugenol binds to surfactant bilayers in vesicles as evident by PRM specific broadening of peaks relevant to alkene and aromatic protons. Chemical structures of these PRMs play a pivotal role in modulating final properties of vesicular dispersions. Understanding their behavior is key to the development of stable formulations with better shelf life.

## 5.2 Introduction

Vesicles are often made up of single or multiple bilayers consisting of surfactants or phospholipids.[1,2] They are promising delivery vehicles for drugs and active ingredients[3-6]. Because of their similarity to biological membranes, vesicles are often used as model systems to probe the impact of biological processes on their stability and structure. In cosmetics, vesicles not only deliver encapsulated ingredients like perfume, but also counter skin dryness as the surfactants are hydrated.[7, 8]

Another important area that extensively uses vesicles is fabric softeners. Cationic surfactants are the chief ingredients of these vesicles.[9-11] During the late stage of

laundry cycle, these cationic surfactants are adsorbed on negatively charged fabric which results in reduction of friction due to exposure of surfactant tails. The inability to form hydrogen bonds also aids reduction of static charge that helps in ironing clothes. Esterquats such as diethy ester dimethyl ammonium chloride (DEEDMAC) are double chained cationic surfactants used mainly as ingredients of these vesicles. Because of ester linkages, these surfactants are readily biodegradable by hydrolysis post washing cycle.[12] Phase diagrams and thermal properties of common double-tailed charged surfactants such as didodecyl dimethyl ammonium bromide[13, 14] (DDAB), dioctadecyl dimethyl ammonium bromide[15, 16] (DODAB) and dioctadecyl dimethyl ammonium chloride [17, 18] (DODAC) in water has shown that in concentration range of 0.15−30 wt % in water and above the main phase transition temperature of the bilayer, such cationic surfactants self assemble to form unilamellar and multilamellar vesicles. In suspensions, these vesicles are believed to exist as a kinetically stabilized metastable phase rather than a thermodynamic equilibrium phase.[19-21]

Fragrance is an integral part of these consumer good products and extended duration of smell is an important product requirement as it determines acceptability by consumers. Perfume raw materials (PRMs) are added to vesicular suspensions which are the key constituent of many consumer products[22] that preserve pleasant odor over long periods of time. An important prerequisite of PRMs is that they should not change the inherent microstructures of the product and do not negatively impact shelf life by destabilization and increase in viscosity. Change in the lamellarity and size of vesicles can modulate the existing balance of buoyancy forces in the suspension. This can lead to destabilization of vesicles in suspension either by creaming or by

sedimentation. Furthermore, this can significantly alter the volume fraction and rheology of a vesicle suspension and in many cases the flow properties represent a crucial design parameter in vesicle-based products.

In this work we look at the impact of PRMs on the structural evolution of vesicular structures in commercial fabric softener, Ultra Downy Free (UDF). Two PRMs linalyl acetate and eugenol are used for this study. We employ time resolved cryogenic transmission electron microscopy to look at microstructural changes and find differences in behavior when these two oils are introduced into the vesicular solution. These transitions are observed over period of 24 hrs. While linalyl acetate doesnot have any impact on the inherent microstructures of UDF, we observe a transition from multi lamellar vesicles to predominantly unilamellar vesicles over a period of time when eugenol is introduced into UDF. We attribute this to the chemical properties of the PRM and their interaction with surfactants in bilayers. Nuclear magnetic resonance is employed to understand specific interactions that lead to these transitions.

## 5.3 Materials

Ultra Downy Free and gentle is obtained from Procter & Gamble. Linalyl acetate (>=97%), acetone(99%), eugenol (99%) are obtained from Sigma Aldrich. Deuterium oxide for NMR (99.9 atom % D) is obtained from Acros Organics. Calcium chloride (anhydrous) is obtained from Alfa Aesar. All materials are used as received.

## 5.4 Methods

### 5.4.1 Sample Preparation for cryo-TEM

UDF is mixed with 1200 PPM calcium chloride solution in a 1:1 volume ratio. 2 wt% PRM is added to this suspension. Probe sonication is used to disperse oil in the

vesicular dispersion of UDF. For this, a Qsonica 125 watt probe sonicator operating at 20kHz and 40% amplitude is used for a period of 2 minutes. The oil mixes immediately. A few microliters of the solution are deposited on to a holey carbon cryo-TEM grid at different time points. The grid is carefully blotted so that liquid bridges of the order of 100 nm in thickness are formed across the holes. It is then plunged into a liquid ethane reservoir cooled by liquid nitrogen. Rapid heat transfer away from the solution on the grid leads to vitrification. Vitrification of samples is an artifact-free way to quench the system, allowing morphology information to be captured at a specific time point. Time is carefully managed so that the sample gets vitrified at a desired time point. This entire operation is done in a controlled environment vitrification system (CEVS) maintained at 25 $^{\circ}$C and at 100% humidity to prevent water evaporation from the sample prior to vitrification.

**5.4.2** Cryo-TEM characterization

The grid-containing sample is transferred to a cooled tip of a Gatan 626 DH cryo transfer stage. The stage is then inserted into a JEOL JEM 2100 Transmission Electron Microscope. The sample is maintained at -175 $^{\circ}$C and low electron dosage is used for probing the samples to prevent the amorphous to crystalline phase transformation in ice as well as any potential dehydration.

**5.4.3** Nuclear Magnetic Resonance

$^{1}$H NMR spectra (300 MHz) are recorded on a Bruker-Advance 300 MHz NMR spectrometer using tetramethylsilane (TMS) as an internal standard. NMR spectra of eugenol (2 wt% in $D_2O$ containing 1200 PPM calcium chloride) are recorded with varying amounts of UDF -2 wt%, 4 wt% over an extended period (3 hrs, 24 hrs). For

experiments with linalyl acetate, 80 vol% stock solution in acetone is first period, followed by dilution with $D_2O$ containing 1200 PPM calcium chloride to a 2 wt% effective concentration of linalyl acetate. This is done as linalyl acetate has very low solubility in water. Experiments are done by sequentially adding UDF to this and monitoring peak intensity and broadening of specific peaks relevant to the PRM.

**5.5 Results and Discussion**

Fig. 1 shows the cryo TEM micrograph of UDF. Vesicles with multiple lamellae are observed as marked by arrows. Double chained DEEDMAC is packed in the bilayers of these lamellae with head groups facing the aqueous phase. The concentration of DEEDMAC in this formulation is in the range of 10 – 12.5 wt%. Change in osmotic pressure outside unilamellar DODAB vesicles has been known to deflate vesicles into cup-like shapes in which poles of the vesicles approach each other until they fuse into a bilamellar twinned vesicles.[23] Similar structural changes have also been observed in DEEDMAC vesicles.[8] Our experiments suggest that when UDF suspension is diluted by 1200 PPM calcium chloride solution in a 1:1 volume ratio the multilamellar structures are preserved indicating an isotonic condition (image not shown).

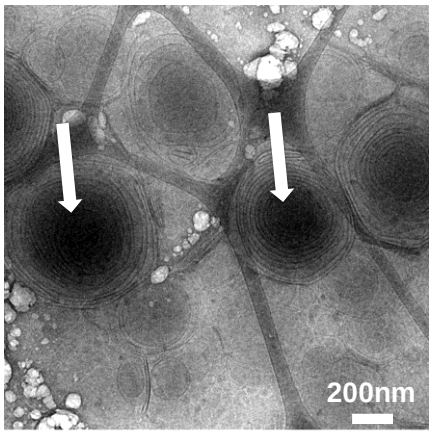


**Figure 1.** Cryo TEM micrograph of Ultra Downy Free (UDF) showing multilamellar vesicles as marked by arrows.

Addition of 2 wt% linalyl acetate (LA) to UDF shows no structural changes in the vesicles. 10 seconds after mixing LA with UDF we see multi lamellar structures as shown in Fig. 2(a). 24 hrs after mixing we see that the multilamellar structures are preserved as shown in Fig. 2(b). Morphology and number of lamellae in these vesicles indicate that if LA is incorporated into the bilayer this does not cause any alteration of the inherent vesicular structures.

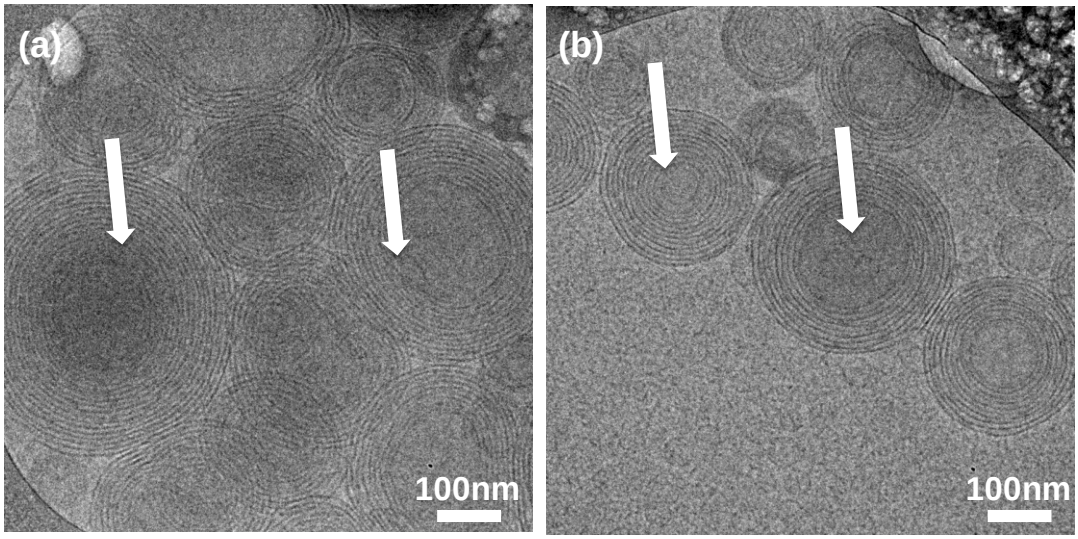


**Figure 2.** Cryo TEM micrographs of UDF with 2 wt% linalyl acetate showing multilamellar vesicles **(a)** 10 seconds after mixing and **(b)** 24 hrs after mixing**.**

When 2wt% eugenol is added to UDF we observe changes in vesicular structures. Immediately after mixing multilamellar vesicles are observed as shown in Fig. 3(a). At 6hrs we start observing instabilities in bilayers. These are indicated by arrows in Fig. 3(b). These instabilities propagate to later stages as shown in Fig. 3(c). The external lamellae break off from the vesicles and bilayer fragments are observed as indicated by arrows at 12hrs after mixing. The inner vesicles follow similar trend. 24hrs after mixing we observe the presence of predominantly unilamellar vesicles, tubules and

bilayer fragments as marked in Fig. 4(a). To confirm morphology of these structures the TEM stage is tilted by an angle of 20° into the plane of the micrograph.

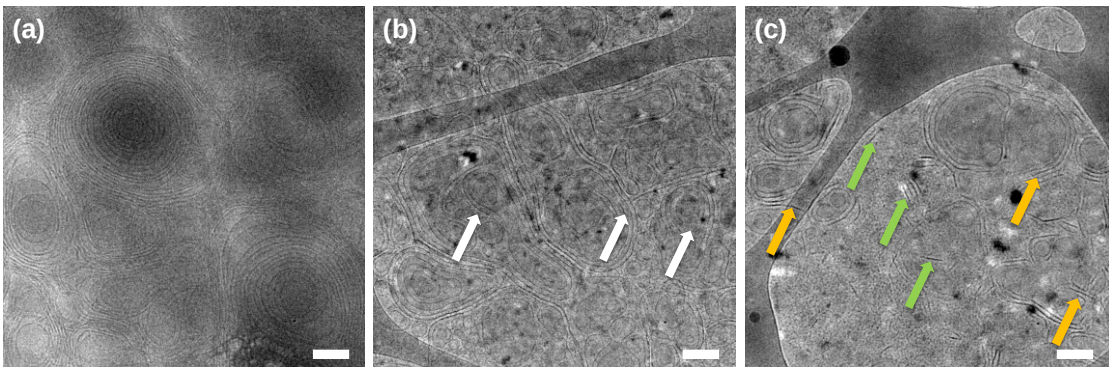


**Figure 3.** Cryo TEM micrographs of UDF with 2 wt% eugenol **(a)** 10 seconds after mixing showing multilamellar vesicles,**(b)** 6hrs after mixing showing instabilities as marked by arrows and **(c)** 12hrs after mixing showing disintegration of bilayers marked by yellow arrows, free bilayer fragments. Scale bars are 100nm.

Fig. 4(b) shows TEM micrograph obtained after stage tilting. While the shape of a tubule remains unchanged after tilting, a bilayer fragment which has shape of a disk, may either appear distinctly or disappear depending whether it is in plane of reference.[24] A transition from multi lamellar vesicles to predominantly unilamellar vesicles is observed over a period of 24 hrs when eugenol is added to UDF. Increase in unilamellar vesicles can lead to vesicle crowding and due to excluded volume, viscosity and hence rheological properties of the suspension can change.[8] Visual inspection of the two samples indicate that the UDF sample with 2 wt% eugenol has an increased viscosity after 24hrs where as the UDF sample with 2 wt% LA has similar flow properties as UDF itself.

While LA has no impact on the vesicular structures, eugenol triggers morphological changes in UDF. This is why LA is labeled as a ‘good’ PRM and eugenol a ‘bad’ PRM. Both of these PRMs have different chemical structures. Packing parameter of a surfactant plays an important role in self assembly into various structures.[2] If a PRM

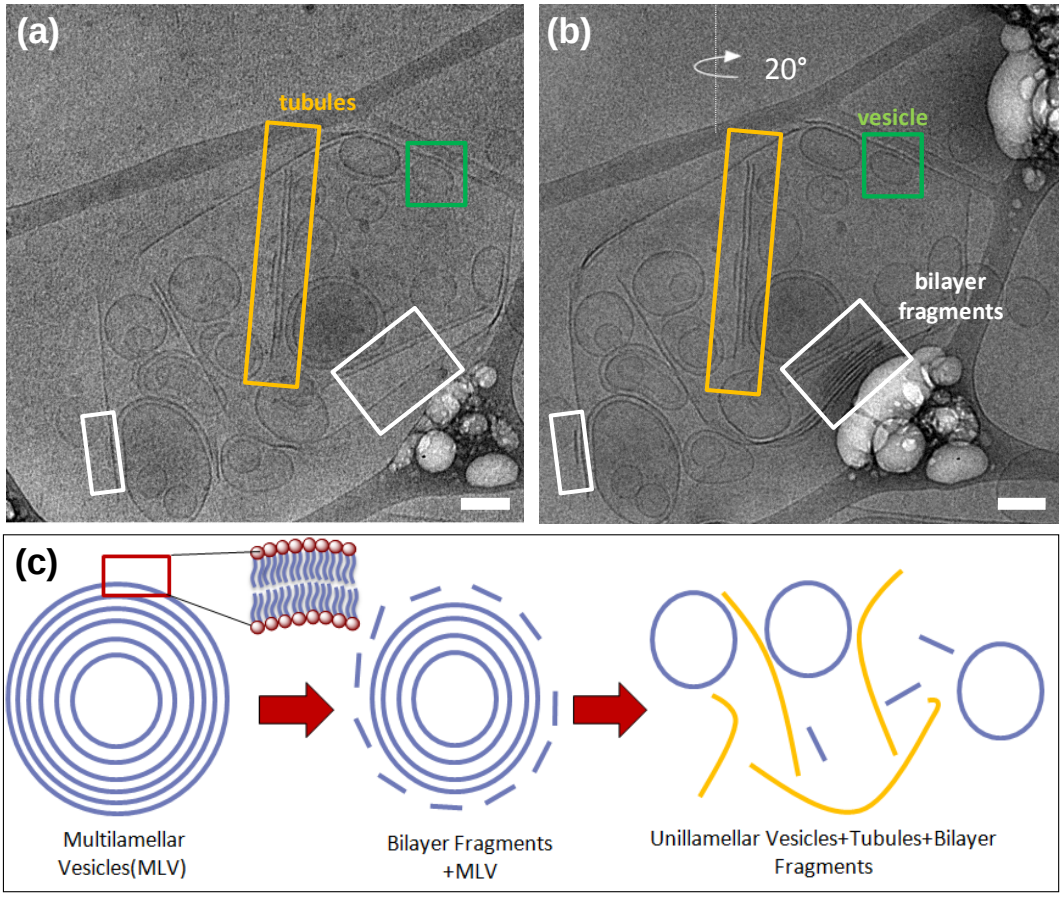


**Figure 4.** Cryo TEM image of UDF mixed with 2 wt % eugenol 24hrs after mixing showing **(a)** unilamellar vesicles, tubules, bilayer fragments and **(b)** morphologies as confirmed by tilting TEM stage by an angle of 20 degrees. Scale bars are 100 nm. **(c)** Schematic showing transition from multilamellar vesicles to predominantly unilamellar vesicles in UDF in the presence of eugenol. Scale bars are 100nm.

is somewhat surface active, then if it gets into the bilayer during mixing, it can interact with surfactant tails of DEEDMAC resulting in bilayer breaking off due to changes in packing parameter. As exposure of surfactant tails to water is energetically unfavorable, these bilayers curl to form unilamellar vesicles.[2, 24] Eugenol has an aromatic ring and a terminal hydroxyl group, which makes it more surface active that LA. In Fig. 4(c), the process of transition from multilamellar vesicles to unilamellar vesicles in UDF is illustrated in the presence of eugenol. LA on the other hand being less surface active could prefer to remain in the bilayer without any specific

association owing to its hydrophobicity or can be phase separated after mixing if it doesnot manage to get into the bilayers.

During last rinsing step of washing cycle using a fabric softener, repartitioning of perfume from vesicles towards the aqueous phase is not desirable as a PRM might get away when the rinse water is pumped away.[7] If the PRM on other hand stays with surfactant, when deposited on the textile it can result in extended duration of odor which is highly desirable in these products. Hence, it is very important to understand if a PRM interacts with DEEDMAC in bilayers of UDF. For this, we employ NMR.

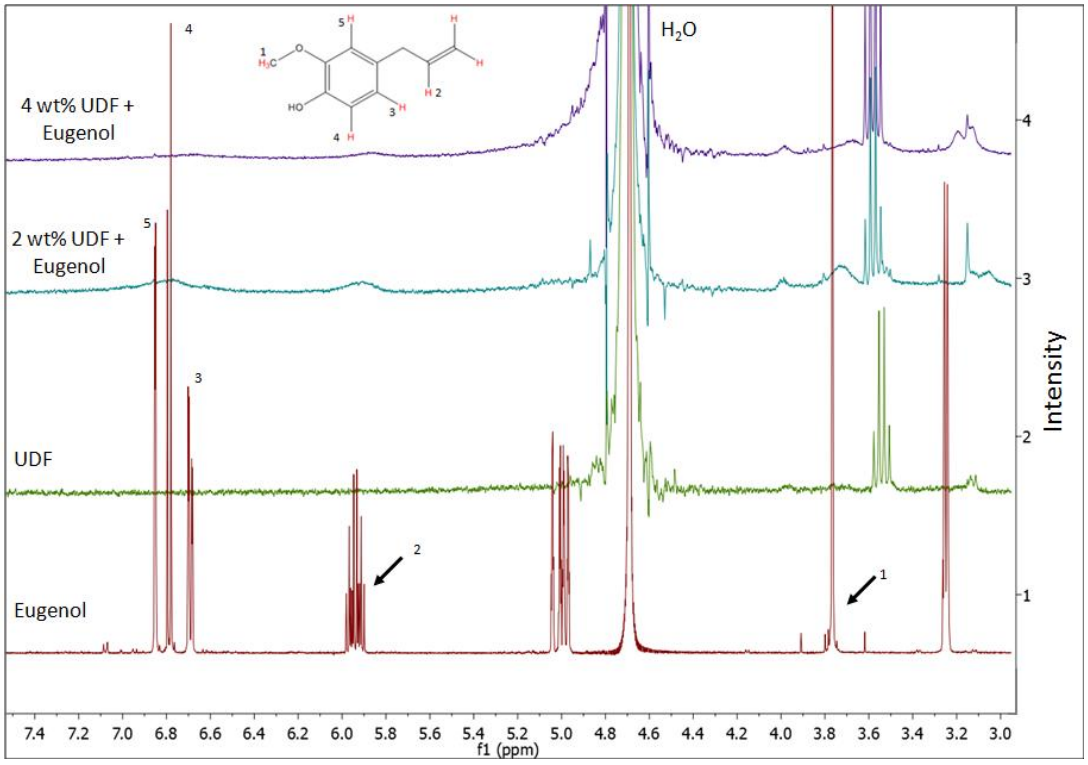


**Figure 5.** NMR spectra showing impact of adding UDF to 2 wt% eugenol in $D_2O$ containing 1200 PPM calcium chloride. Broadening of marked peaks is seen. These peaks correspond to the tracked protons marked by red color and numbers in the chemical structure of eugenol.

Addition of 2 wt% or 4 wt% UDF to a 2 wt% eugenol suspension in $D_2O$ containing 1200 PPM calcium chloride exhibit peak broadening at chemical shifts 3.75 ppm (methoxide protons, 5.9 ppm (vinyl proton) and 6.75 ppm (aromatic protons) as shown

in NMR spectra in Fig. 5. These measurements are done 3 hrs after mixing. This can be explained as association of eugenol with DEEDMAC in vesicle bilayers. Spectra are also obtained at 24 hrs after mixing for the sample where 2 wt% UDF is added to 2 wt% eugenol suspension in $D_2O$. Fig. 6 shows that for chemical shifts 5.9 ppm, 6.75 ppm which correspond to vinyl and aromatic protons respectively, the integral values of peaks in question increase with time. The integrations of NMR peaks are the relative areas under the curve measured against a calibrated internal standard corresponding to a residual $H_2O$ peak at 4.79 ppm (calibrated to 100). Over time an

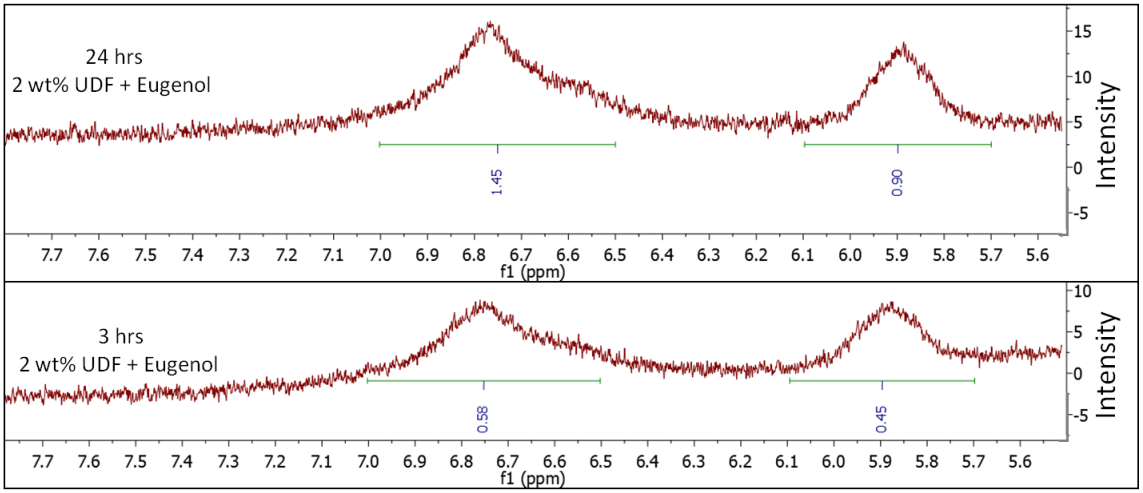


**Figure 6.** NMR spectra tracking specific protons during the addition of 2 wt% UDF in eugenol, showing increase in integral at 24 hrs as indicated by green colored bars. This indicates that some eugenol could have been released to the aqueous environment during bilayer breaking off process.

increase in integral indicate that some eugenol leaves the bilayers and are released into water during the bilayer breaking off process as observed in TEM micrographs and proposed in our model. Fig. 7 shows NMR spectra of 2 wt% LA in $D_2O$ containing 1200 PPM calcium chloride when exposed to 4 wt% UDF over a period of 24 hrs. NMR peaks, at chemical shifts 1.38 ppm, 1.45ppm, 1.54ppm, 1.79ppm which represent methyl protons remain unchanged showing no association with vesicles in

UDF. Similar behavior is also observed for the multiplets of alkene protons at chemical shifts 5.1 ppm and 5.8 ppm.

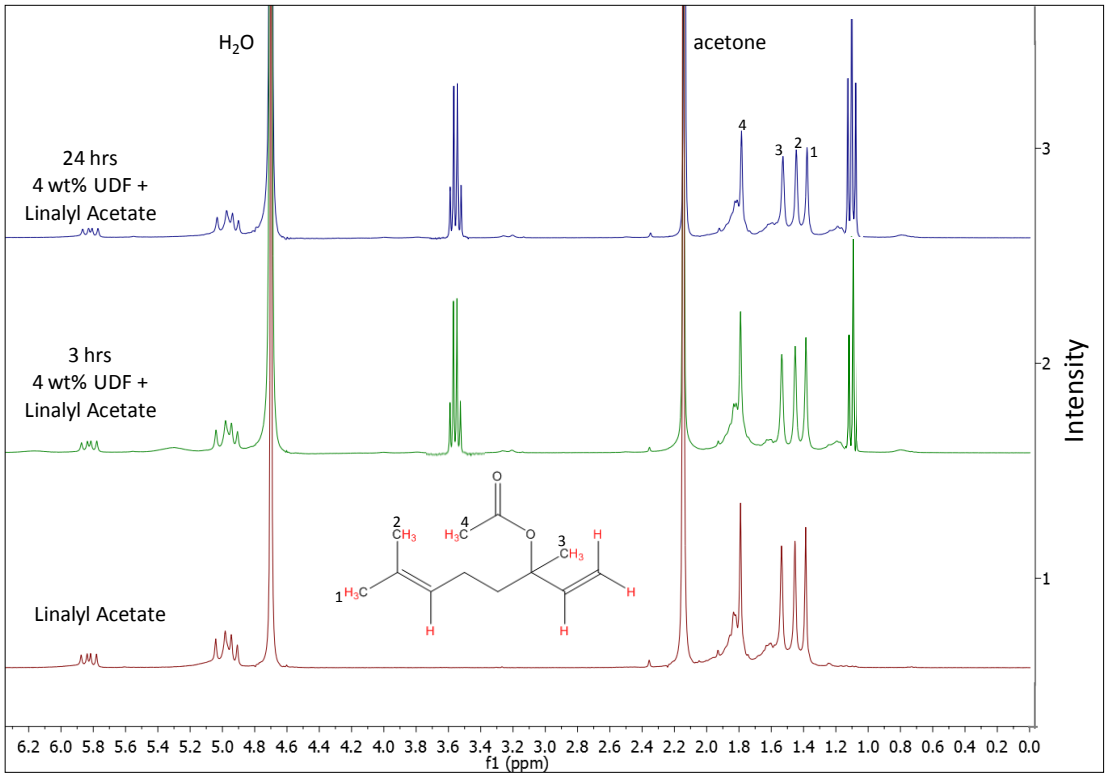


**Figure 7.** NMR spectra showing addition impact of adding 2 wt % UDF to linalyl acetate showing that the intensity of marked peaks remain sharp and their intensity remains almost same over time. No peak broadening is observed.

## 5.6 Conclusions

We demonstrate that addition of perfume raw materials (PRM) to a vesicular dispersion of commercial fabric softener, Ultra Downy Free (UDF) results in structural changes. We attribute this to the interaction between a PRM molecule with surfactant bilayer in UDF. Time resolved cryogenic transmission electron microscopy is used to probe these transitions. While 2 wt% linalyl acetate (LA) does not alter the multi lamellar vesicular structures, addition of same amount of eugenol triggers a series of structural changes which result in a transition from multi lamellar to predominantly uni lamellar vesicles through a bilayer breakage process. This results in

increased viscosity of UDF. Nuclear magnetic resonance experiments show that addition of UDF to eugenol results in peak broadening reminiscent of association or attachment to the bilayer. Over time the intensity of these peaks increase indicating possible release to surrounding aqueous environment during bilayer breakage while transitioning to uni lamellar vesicles. Understanding PRM interaction with vesicular structures is key to developing stable, aesthetically appealing products desired by consumers.

**5.7 Acknowledgements**

We gratefully acknowledge the financial support provided by Procter & Gamble, Cincinnati, OH 45202.

**References**

1. Seifert, U., Configurations of fluid membranes and vesicles. *Advances in Physics* **1997,** 46, (1), 13-137.

2. Israelachivili, J. N., *Intermolecular and surface forces*. Second ed.; Academic Press: 2005.

3. Schreier, H.; Bouwstra, J., Liposomes and niosomes as topical drug carriers: dermal and transdermal drug delivery. *Journal of Controlled Release* **1994,** 30, (1), 1-15.

4. Walde, P.; Ichikawa, S., Enzymes inside lipid vesicles: preparation, reactivity and applications. *Biomolecular Engineering* **2001,** 18, (4), 143-177.

5. Sakai, H.; Tsuchida, E., Hemoglobin-vesicles for a Transfusion Alternative and Targeted Oxygen Delivery. *Journal of Liposome Research* **2007,** 17, (3-4), 227-235.

6. Pohorille, A.; Deamer, D., Artificial cells: prospects for biotechnology. *Trends in Biotechnology* **2002,** 20, (3), 123-128.

7. Heynderickx, P. M.; De Clercq, S.; Saveyn, P.; Dewulf, J.; Van Langenhove, H., Determination of the sorption and desorption kinetics of perfume raw materials in the liquid phase with vesicular dispersion: Application of SIFT-MS. *Chemical Engineering Journal (Amsterdam, Netherlands)* **2013,** 217, 281-288.

8. Seth, M.; Ramachandran, A.; Murch, B. P.; Leal, L. G., Origins of Microstructural Transformations in Charged Vesicle Suspensions: The Crowding Hypothesis. *Langmuir* **2014,** 30, (34), 10176-10187.

9. Obendorf, S. K., Electron microscopic analyses of the distribution of oily soils on fabrics after laundering: a review. *Journal of Coated Fabrics* **1983,** 13, (1), 24-34.

10. Obendorf, S. K.; Dixit, V.; Woo, D. J., Microscopy Study of Distribution of Laundry Fabric Softener on Cotton Fabric. *Journal of Surfactants and Detergents* **2009,** 12, (3), 225-230.

11. Obendorf, S. K.; Solbrig, C. M., Distribution of malathion and methyl parathion on cotton/polyester unfinished and durable-press fabrics before and after laundering as determined by electron microscopy. *ASTM Special Technical Publication* **1986,** 900, (Perform. Prot. Clothing), 187-204.

12. Giolando, S. T.; Rapaport, R. A.; Larson, R. J.; Federle, T. W.; Stalmans, M.; Masscheleyn, P., Environmental fate and effects of DEEDMAC: a new rapidly biodegradable cationic surfactant for use in fabric softeners. *Chemosphere* **1995,** 30, (6), 1067-83.

13. Dubois, M.; Zemb, T., Phase behavior and scattering of double-chain surfactants in diluted aqueous solutions. *Langmuir* **1991,** 7, (7), 1352-60.

14. Marques, E. F.; Regev, O.; Khan, A.; Miguel, M. d. G.; Lindman, B., Vesicle formation and general phase behavior in the catanionic mixture SDS-DDAB-water. The cationic-rich side. *Journal of Physical Chemistry B* **1999,** 103, (39), 8353-8363.

15. Svitova, T. F.; Smirnova, Y. P.; Pisarev, S. A.; Berezina, N. A., Self-assembly in double-tailed surfactants in dilute aqueous solutions. *Colloids and Surfaces, A: Physicochemical and Engineering Aspects* **1995,** 98, (1/2), 107-15.

16. Haas, S.; Hoffmann, H.; Thunig, C.; Hoinkis, E., Phase and aggregation behaviour of double-chain cationic surfactants from the class of N-alkyl-N-alkyl'-N,N-dimethylammonium bromide surfactants. *Colloid and Polymer Science* **1999,** 277, (9), 856-867.

17. Feitosa, E.; Karlsson, G.; Edwards, K., Unilamellar vesicles obtained by simply mixing dioctadecyldimethylammonium chloride and bromide with water. *Chemistry and Physics of Lipids* **2006,** 140, (1-2), 66-74.

18. Laughlin, R. G.; Munyon, R. L.; Fu, Y. C.; Fehl, A. J., Physical science of the dioctadecyldimethylammonium chloride-water system. 1. Equilibrium phase behavior. *Journal of Physical Chemistry* **1990,** 94, (6), 2546-52.

19. Laughlin, R. G., Equilibrium vesicles: fact or fiction? *Colloids and Surfaces, A: Physicochemical and Engineering Aspects* **1997,** 128, (1-3), 27-38.

20. Luisi, P. L., Are micelles and vesicles chemical equilibrium systems? *Journal of Chemical Education* **2001,** 78, (3), 380-384.

21. Pansu, R. B.; Arrio, B.; Roncin, J.; Faure, J., Vesicles versus membrane fragments in DODAC suspensions. *Journal of Physical Chemistry* **1990,** 94, (2), 796-801.

22. Jefferson, B. Customized disposable hand towel and method. 2013-13751703 20140033557, 20130128., 2014.

23. Hubert, D. H. W.; Jung, M.; Frederik, P. M.; Bomans, P. H. H.; Meuldijk, J.; German, A. L., Morphology Transformations of DODAB Vesicles Reminiscent of Endocytosis and Vesicular Traffic. *Langmuir* **2000,** 16, (23), 8973-8979.

24. Hiemenz, P., C., *Principles of Colloid and Surface Chemistry*. Second ed.; New York and Basel, 1986.